

# UCLA

## UCLA Previously Published Works

### Title

High-Efficiency Production of Radiopharmaceuticals via Droplet Radiochemistry: A Review of Recent Progress

### Permalink

<https://escholarship.org/uc/item/9mn1712x>

### Authors

Wang, Jia  
van Dam, R Michael

### Publication Date

2020

### DOI

10.1177/1536012120973099

### Copyright Information

This work is made available under the terms of a Creative Commons Attribution-NonCommercial License, available at <https://creativecommons.org/licenses/by-nc/4.0/>

Peer reviewed

# High-Efficiency Production of Radiopharmaceuticals via Droplet Radiochemistry: A Review of Recent Progress

Jia Wang, PhD<sup>1</sup>  and R. Michael van Dam, PhD<sup>1</sup> 

## Abstract

New platforms are enabling radiochemistry to be carried out in tiny, microliter-scale volumes, and this capability has enormous benefits for the production of radiopharmaceuticals. These droplet-based technologies can achieve comparable or better yields compared to conventional methods, but with vastly reduced reagent consumption, shorter synthesis time, higher molar activity (even for low activity batches), faster purification, and ultra-compact system size. We review here the state of the art of this emerging direction, summarize the radiotracers and prosthetic groups that have been synthesized in droplet format, describe recent achievements in scaling up activity levels, and discuss advantages and limitations and the future outlook of these innovative devices.

## Keywords

advances in PET/SPECT probes, novel chemistry methods and approaches, lab-on-a-chip devices, PET, radiochemistry

## Introduction

As a molecular imaging technique, positron-emission tomography (PET) provides *in vivo* information about the rates of specific biomolecular processes or distribution of biological targets. PET has wide applications in the study of disease, drug development, disease diagnosis, monitoring response to treatment, and recently, individualized dosimetry for theranostics.<sup>1-6</sup> PET requires injection of tiny, non-pharmacologic amounts of radiotracers (e.g., small molecules, peptides or proteins labeled with positron-emitting radioisotopes) that accumulate in target regions throughout the body. Then, the distribution of the radiotracer is reconstructed from observation of many decay events with a PET scanner.

Production of these tracers is carried out primarily using specialized automated radiosynthesizers that operate within radiation-shielded “hot cells” to perform multi-step synthesis protocols in milliliter-scale volumes. Due to the short half-life of commonly-used radioisotopes (e.g. 110 min for fluorine-18), the shelf-life of positron-emitting tracers is limited (e.g. a few hours for <sup>18</sup>F-labeled tracers), and therefore their production must be carried out near the location where they will be used, and the production must occur just before use. For commonly used tracers (e.g., [<sup>18</sup>F]FDG), a manufacturing site

(radiopharmacy) can produce large batches and divide them up into many individual patient doses that are transported to nearby imaging facilities, resulting in a relatively low cost per dose. However, for most other tracers, the demand is currently relatively low, and it may be impossible to schedule multiple end users at the same time, resulting in a single dose costing as much as the full batch; for many applications such as preclinical research, and development/validation of novel tracers, the cost of producing or obtaining the tracer can be prohibitive.

In recent years, numerous microfluidic-based radiosynthesizers have emerged,<sup>7,8</sup> which have the potential to lower the production cost and increase accessibility of tracers via orders of magnitude reduction in consumption of expensive reagents (via volume reduction from milliliter-scale to microliter-scale),

<sup>1</sup> Crump Institute for Molecular Imaging and Department of Molecular and Medical Pharmacology, David Geffen School of Medicine, University of California Los Angeles, Los Angeles, CA, USA, Los Angeles, CA, USA

Submitted: 16/06/2020. Revised: 02/09/2020. Accepted: 12/10/2020.

## Corresponding Author:

R. Michael van Dam, UCLA Crump Institute for Molecular Imaging 570 Westwood Plaza, Los Angeles, CA 90095, USA.

Email: mvandam@mednet.ucla.edu



faster and simplified synthesis processes, and dramatically smaller footprint of the apparatus. Often these devices can be implemented with a disposable fluid path that reduces the need for cleaning and reduces concerns about chemical or radiation damage to system components.

One category of microfluidic radiosynthesizers is based on “flow chemistry,” in which reagent streams flow through a mixer and a thermally-controlled capillary or channel (and possibly additional stages for multi-step reactions). Flow systems have highly uniform conditions within the reactor due to rapid mixing and high surface-to-volume ratio, and reactions have been observed to be very fast.<sup>9-11</sup> Using custom built and commercial flow systems, a wide range of different PET and SPECT tracers have been synthesized, including molecules labeled with fluorine-18, carbon-11, nitrogen-13, technetium-99, copper-64, zirconium-89, gallium-68, and lutetium-177.<sup>12-16</sup> In these systems, some steps of the tracer production process are performed using conventional macroscale setups (i.e., drying and activation of [<sup>18</sup>F]fluoride upstream of the flow reaction, and purification of the crude tracer downstream of flow reaction), though some efforts have been made to implement them in a flow-like format.<sup>17-20</sup> Some flow systems can perform reactions using just 10 s of microliters for optimization purposes, resulting in low reagent and precursor consumption. While scaling up the activity of the product often involves scaling up the volumes of both the radioisotope solution and precursor solution, using amounts on par with conventional systems for larger-scale tracer production, scaling can alternatively be achieved by increasing the concentration of the radioisotope solution prior to introduction into the flow reactor to avoid the increase in precursor consumption. For example, electrode-based [<sup>18</sup>F]fluoride trap and release cells implemented in microfluidic format show the potential to increase activity concentration and to be integrated with flow microreactors.<sup>21,22</sup>

The other major category of microfluidic systems are “batch” reactors, which perform reactions at the 10 s of microliter scale or smaller (as low as 40 nL has been reported<sup>23</sup>). Often there is a higher degree of process integration in these devices, such as the capability to perform the upstream [<sup>18</sup>F]fluoride drying and activation process in the same place as the subsequent reaction step(s). These very compact systems that can potentially be operated with local shielding and without the need for hot cells, within or nearby imaging centers, for on-demand production of tracers. Some efforts aimed at integrating the purification step have also been reported.<sup>24-26</sup> The reaction volume and quantity of reagents is typically conserved in batch reactors even when the activity is scaled up. The small reaction volume can lead to significant reductions in precursor consumption (often ~10-100x less than conventional radiosynthesis). It also leads to improved molar activity in <sup>18</sup>F-radiosyntheses due to reduction of reagents (which are the major source of <sup>19</sup>F-contamination),<sup>27</sup> and enables high molar activity of <sup>18</sup>F/<sup>19</sup>F isotopic-exchange reactions (due to minimal amount of precursor in the reaction).<sup>28</sup>

Though a variety of different batch microfluidic approaches for labeling with fluorine-18, gallium-68, and nitrogen-13 have been reported in the last few years<sup>26,29-33</sup> that highlight these advantages, including droplet reactors, small microfluidic reaction chambers,<sup>26</sup> and specialized small conical vials,<sup>33</sup> we focus in this review on droplet-based methods in particular. In 2015, we reviewed the initial emergence of droplet reactors based on electrowetting-on-dielectric (EWOD) in the field of radiochemistry.<sup>34</sup> Significant progress has been made in the last several years including development of new types of droplet-based radiosynthesis platforms with improved synthesis performance and reliability, decreased chip costs, faster operation, and expanded range of applications through increased variety of tracers and increased synthesis scale. We describe each droplet radiochemistry platform, review the radiolabeled compounds that have been made in droplet format, summarize the advantages of droplet-based methods, and describe recent efforts to scale up the activity. Finally, we discuss the outlook for these technologies and the potential for integration into mainstream radiochemistry practice.

## Emerging Droplet-Based Radiosynthesizers

We first describe the different platforms that have been reported in recent years for performing radiochemistry in small-volume droplets (summarized in Figure 1).

### Electrowetting-on-Dielectric (EWOD)

EWOD chips are composed of 2 substrates between which droplets are sandwiched (Figure 1A). The bottom layer has a set of electrodes, covered by a dielectric layer and a chemically inert hydrophobic layer (Teflon AF), while the cover chip typically has a single, large ground electrode and a hydrophobic coating.<sup>35</sup> Droplet movement from reagent pipetting sites at the periphery to the central reaction zone is realized by activating in sequence a series of buried electrodes, which act as a virtual channel. Localized heating of the reaction region is provided by passing current through heating electrodes on the chip surface, and mixing can be carried out by using the heaters as actuation electrodes. When performing solvent evaporation, a nitrogen flow is applied in conjunction with heating to drive the vapor out of the chip. After the reaction step(s), the product is collected via pipette. Initially-reported chips measured 38 mm × 51 mm with a capacity of the reaction site of up to 17 μL.<sup>38</sup> Electrical contacts along the edges of the chip connect to the control system, which was located outside of the radiation shielding. We previously reviewed this technology and its application to the synthesis of several <sup>18</sup>F-labeled compounds.<sup>34</sup>

After our group established initial proof-of-concept, extensive efforts were made in collaboration with Sofie, Inc. (Culver City, CA) to shrink the electronic apparatus, and to lower the chip cost and boost reliability (via smaller chip size and new fabrication and testing methods<sup>39</sup>). The optimized chip measured 25 mm × 25 mm and reactions were performed in up to 10 μL volumes. On-chip heater electrodes were removed from

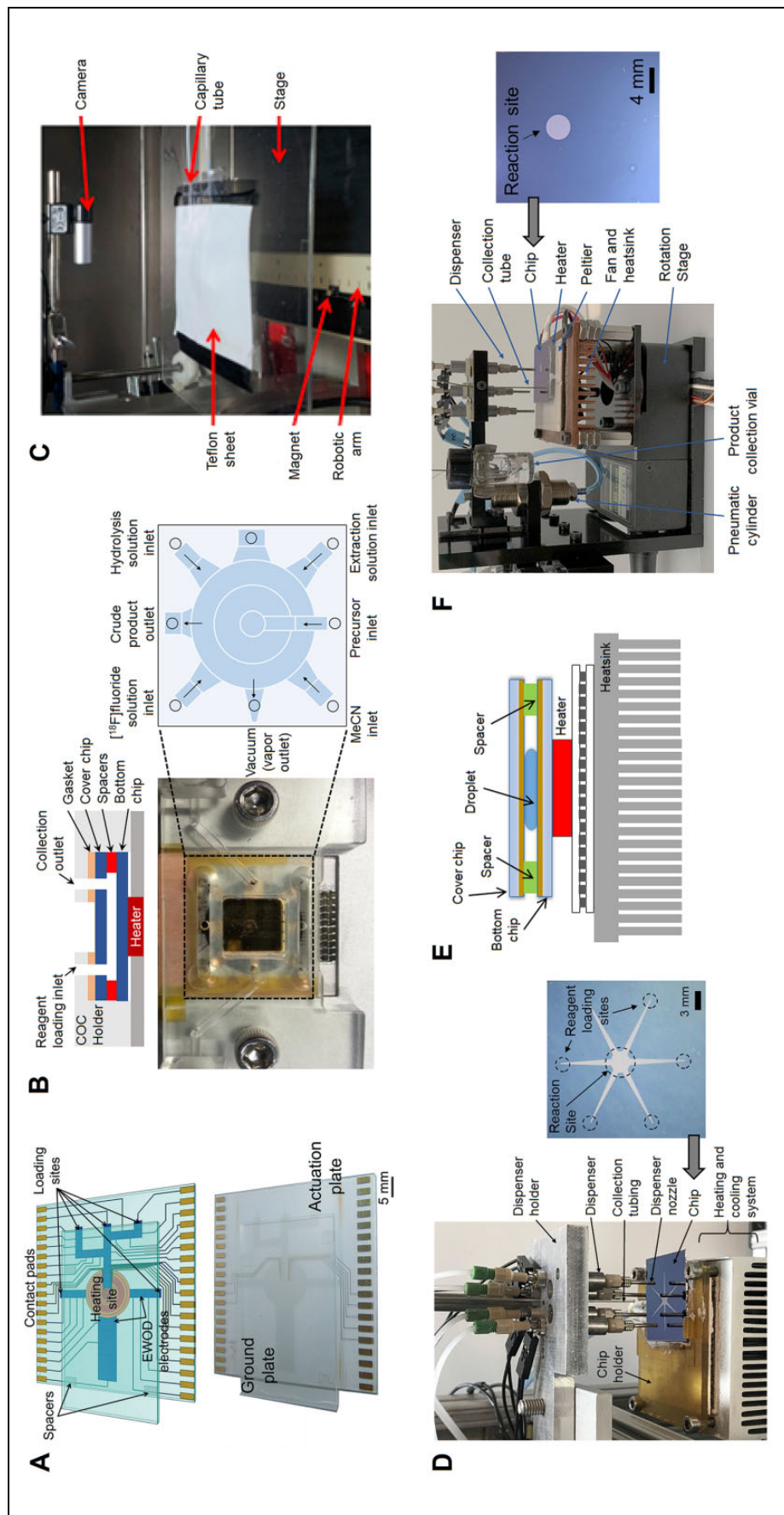


**Figure 1.** Platforms reported for performing radiochemistry in droplet format. **A**, Schematic (top) and photography (bottom) of EWOD-based radiosynthesis chip. Reactions take place in droplets sandwiched between the chip substrate (actuation plate) and cover (ground plate). Reagents are deposited at the edge of the chip and transported via actuation electrodes to the central reaction site where heating electrodes are integrated. Reproduced from Chen et al.<sup>35</sup> with permission from The Royal Society of Chemistry. **B**, Second-generation EWOD-based radiosynthesis platform. (Top) Cross-section of the chip installed in a disposable cassette. The chip contacts the temperature-controlled heater on its bottom surface and is clamped down by a cyclic olefin copolymer (COC) cover plate containing channels and pumps that interfaces with the inlet and outlet ports of the chip for automated reagent delivery and product collection. (Right) Universal mapping of inlet and outlet holes for radiosynthesis. EWOD actuation electrodes are shown in blue. Electrical contact pads and connection lines are omitted for clarity. **C**, MDM platform. Reactions take place in droplets deposited on top of a Teflon sheet. Droplets are manipulated via the addition of magnetic particles, which are controlled via a magnet below the Teflon sheet mounted to a robotic arm. When needed, solvent is removed via suction by a capillary tube rather than by evaporation. Adapted from Fiel et al.<sup>36</sup> with permission from American Chemical Society, Copyright © 2015. **D**, Radiosynthesis platform based on passive transport of droplets via patterned wettability. The platform provides automated temperature control of the chip, delivery of reagents, and collection of product. Inset photograph shows the detailed chip design (top view). Adapted from Wang et al.<sup>37</sup> with permission from The Royal Society of Chemistry. **E**, Schematic of the Teflon coated glass chip and the heating setup. Reagent delivery and product collection are performed manually. Adapted from Lisova et al.<sup>28</sup> with permission from Elsevier Inc., copyright © 2018. All rights reserved. **F**, Radiosynthesis platform based on surface-tension trap chips. The platform provides temperature control of the chip, and a rotary actuator to position the reaction site under different reagent dispensers or under the collection tube. Inlet photograph shows the detailed chip design (top view). Adapted from Wang et al.<sup>32</sup> with permission from The Royal Society of Chemistry.

the chip design and replaced with an off-chip heater to improve temperature uniformity. The degree of automation was also improved in this second-generation EWOD platform by mounting the EWOD chip onto a disposable reagent cassette (Figure 1B). The cassette contained pumps to deliver reagents to the chip via holes in the cover plate, a vacuum port to collect vapor condensate during evaporation steps, and a second vacuum port to collect crude product following the synthesis.

Despite the versatility of EWOD, and its high degree of integration and compact size, the high chip complexity and cost hindered more widespread use. In addition, it was difficult to deposit defect-free dielectric films during microfluidic chip fabrication, which could lead to electrolysis and/or droplet pinning during operation, and ultimately reduced reaction yield and product recovery from the chip.

### *Magnetic Droplet Microfluidics (MDM)*

Another platform reported for conducting droplet-based radiosynthesis is based on magnetic actuation.<sup>36</sup> At the beginning of the synthesis, a volume of [<sup>18</sup>F]fluoride solution (up to 1 mL) and droplets of reagents (~50 µL) are manually placed atop a hydrophobic Teflon sheet mounted on plastic stage. By addition of magnetic particles into a droplet, that droplet can be manipulated by robotically moving a magnet mounted under the stage (Figure 1C). Functionalized magnetic particles also serve the function of typical QMA cartridges for [<sup>18</sup>F]fluoride trapping and solvent exchange with the help of a small capillary located in one corner of the sheet, where suction is applied to remove the solution while leaving behind the beads. The beads were mixed with eluent and precursor to perform the reaction, after which the crude product was collected manually via syringe. No method of applying heat was reported in this platform.

While this platform is suitable for moving aqueous droplets and performing room temperature reactions under aqueous conditions (mixture of water and t-BuOH), the ability to extend to additional radiosyntheses involving other organic solvents, elevated temperatures, or moisture-sensitive precursors has yet to be demonstrated.

### *Passive Droplet Manipulation*

In an attempt to circumvent some of the challenges and complexities encountered with active droplet manipulations, our lab developed a droplet-based radiosynthesizer based on passive transport (PT) of droplets.<sup>31</sup> The chip (25.0 mm × 27.5 mm) was made from silicon (hydrophilic) and a Teflon AF coating (hydrophobic). The Teflon coating was etched away to expose 6 radially-oriented hydrophilic reagent delivery channels converging on one central circular hydrophilic reaction site (Figure 1D). The tapered shape of the delivery channels results in a spontaneous driving force on droplets toward the wider end of the taper, thus moving droplets deposited atop the chip at the periphery toward the central reaction site.

The chip was mounted on a temperature control platform comprising a ceramic heater for heating and a thermoelectric

device mounted on a heatsink and fan for cooling. Additional subsystems provided automatic reagent loading, and product collection. During the synthesis, reagents were deposited to the chip on demand using piezoelectric non-contact dispensers, each connected to a pressurized reagent vial. These droplets spontaneously moved to the reaction site and the chip was then heated to perform the desired radiochemistry step. Product collection was achieved by lowering a small stainless steel diptube into the droplet (using a pneumatic actuator) after loading droplets of collection solution. The droplet was transferred through the tube to a product vial by application of vacuum.

Compared to EWOD, the PT chips were significantly simpler resulting in a much lower fabrication cost. Furthermore, without electrodes (or dielectric layer), the chips operated reliably without the risk of electrical breakdown. The use of an external heater not only simplified the chip but resulted in more uniform temperature distribution across the chip, and the high-powered heater enabled temperature increase of the chip from room temperature to the reaction temperature in <10 s. Evaporation steps (e.g. to dry [<sup>18</sup>F]fluoride) were also much faster in the open droplet compared to the covered configuration of EWOD. When performing heated reactions, solvent could be replenished periodically to compensate for any undesired evaporation. However, due to the use of non-contact dispensers and a vertically-actuated collection tube, the size of the system was slightly larger than the EWOD platform.

Although synthesis performance was high (see next section), it proved time-consuming to optimize synthesis protocols because different solvents exhibited different behavior on the chip. For example, a 0.5 µL droplet of DI water just barely filled the central reaction site, while the same volume droplet of DMSO filled the reaction zone but also “overflowed” along all of the delivery channels. To avoid adverse effects on the performance and reliability of the radiosynthesis process, the volume of each reagent and frequency of dispensing had to be carefully considered.<sup>31</sup>

### *Direct Dispensing to Droplet Reaction Site*

In early work with the EWOD platform, many reports described some experiments performed by manually depositing reagents (with micro-pipette) directly onto a designated region of a glass chip (25 mm × 25 mm) with uniform Teflon-AF coating. Elimination of electrodes and dielectric layer provided a chip surface similar to EWOD but significantly reduced the fabrication cost and thus was a valuable approach for synthesis optimization.<sup>40-43</sup> These simple Teflon-glass chips could in fact also be used for manually carrying out the entire production of tracers for imaging.<sup>28,44</sup> Heating was provided by placing the chip atop a temperature control platform (Figure 1E). Typically, radioisotope drying was performed with the chip in an open configuration (no cover), while reaction steps were performed by adding the needed reagents, then adding a cover to sandwich the droplet (using physical spacers to control the height of droplet). Some limitations of this approach are the high degree of manual intervention required, the need to

carefully level the platform and the chip to avoid unwanted migration of droplets, and the care needed to avoid damaging the chip surface with the pipette.

More recently, a new approach was developed by our group, in which the chip consists of Teflon-coated silicon substrate with a circular region (4 mm in diameter) etched out of the Teflon to expose the hydrophilic silicon surface.<sup>32</sup> The hydrophilic site serves as a surface tension trap (STT) that “confines” the reaction droplet, preventing unwanted spreading out or movement (Figure 1F). While similar to the central part of the PT-based chips, the elimination of the tapered hydrophilic channels eliminates problems related to solvent-specific behavior of droplets, simplifying optimization and resulting in excellent synthesis performance with high repeatability. To perform syntheses on this chip in an automated fashion, a compact module about the size of a small coffee cup was developed.<sup>32</sup> The chip was mounted on a temperature control platform which in turn was mounted off-center on a compact rotation stage, which was used to align the reaction site under different reagent dispensers or product collection tubing. Piezoelectric dispensers were used to load reagent droplets directly onto the reaction site. After the chip was heated to perform an evaporation or reaction step, the chip was then rotated to align the reaction site under the dispenser containing the next reagent to be added. Once the synthesis was finished, the resulting crude product was collected by aligning the reaction site under a stainless-steel tube and transferring the droplet off of the chip via application of vacuum.

This platform has many similarities to the PT platform, in terms of size, cost, and complexity of the chip and the overall synthesis platform, with the main advantage being the more consistent containment of droplets at the surface tension trap, leading to faster optimization and improved performance.

### Emerging Active Droplet Manipulation Technologies

Separate from applications in droplet radiochemistry, a variety of exciting new approaches are emerging in the field of “digital microfluidics” for active droplet manipulation. These techniques could potentially address the practical reliability issues experienced with EWOD chips or avoid the bulky motion actuator needed in the MDM platform. For example, a new electro-dewetting approach uses chips containing electrodes similar to EWOD chips, but does not have dielectric or hydrophobic layers, instead relying on a small amount of surfactant added to the droplets to enable manipulation via electric current.<sup>45</sup> These chips are expected to have the same functionality as EWOD, but with lower cost and higher reliability, and further investigation in the context of radiochemistry is warranted. Other than this approach, a wide variety of other forces have been leveraged to provide active droplet manipulation including optoelectrowetting (via deposition of a photoconductive layer),<sup>46</sup> thermocapillary forces (via embedded thin film microheaters),<sup>47</sup> surface acoustic waves (via integration of a piezoelectric substrate),<sup>48</sup> and magnetic forces (via a variety of mechanisms),<sup>49,50</sup> to name just a few. To employ these new

approaches in the radiochemistry field would require investigations of (i) compatibility with elevated temperatures, (ii) ability to transport organic solvents, (iii) compatibility with salt solutions, acids, and bases, (iv) compatibility of radiochemical reactions with the needed additives (e.g. surfactant, magnetic particles, etc.). However, such approaches may enable a greater degree of integrated functionality (with less need for external motion actuators) and potentially even smaller and more reliable overall apparatus.

The characteristics and advantages of each droplet-based radiosynthesizer described above are presented in Table 1. As a summary, all platforms had a capability for remote droplet manipulation on the chip (or did not require droplet manipulation), but differed in the degree of automation of other aspects such as reagent loading and product collection. Except for the MDM approach, all platforms incorporated a heating mechanism and were shown to be compatible with reactions in organic solvents, providing versatility for a broad range of reactions. Due to the open (MDM, PT, STT) or semi-open (EWOD, Teflon-glass) architecture of all droplet approaches, there can be significant evaporation, but the effects can be mitigated by replenishing the solvent periodically (provided the reagents or product are not volatile species).

### Production of Radiopharmaceuticals on Droplet-Based Radiosynthesizers

A wide range of tracers labeled with [<sup>18</sup>F]fluoride have been synthesized using droplet-based radiosynthesizers. A comprehensive summary is included in Table 2.

Most of these tracers were prepared via nucleophilic fluorination routes and require an anhydrous reaction environment, including [<sup>18</sup>F]Fallypride, 2-[<sup>18</sup>F]fluoro-2-deoxy-D-glucose ([<sup>18</sup>F]FDG), 3'-deoxy-3'-[<sup>18</sup>F]fluorodthymidine ([<sup>18</sup>F]FLT), N-succinimidyl-4-[<sup>18</sup>F]fluorobenzoate ([<sup>18</sup>F]SFB), O-(2-[<sup>18</sup>F]fluoroethyl)-L-tyrosine ([<sup>18</sup>F]FET), 3,4-dihydroxy-6-[<sup>18</sup>F]fluoro-L-phenylalanine ([<sup>18</sup>F]FDOPA) and [<sup>18</sup>F]Florbetaben ([<sup>18</sup>F]FBB). The synthesis procedure for all of these compounds was similar across the various droplet platforms: EWOD chips (Figure 2), PT-based chips (Figure 3), Teflon-coated glass chips, and STT-based chips (Figure 4). First, a [<sup>18</sup>F]fluoride/[<sup>18</sup>O]H<sub>2</sub>O droplet premixed with phase transfer catalyst was loaded on the chip and heated to evaporate the water. In EWOD chips, condensation was observed to form nearby the reaction site due to the cooler temperature of the chip away from the heaters at the reaction site. Nitrogen flow between the chip substrates reduced the amount of condensation and accelerated drying. Azeotropic distillation steps (consisting of adding then evaporating acetonitrile) were then performed to ensure thorough removal of water from the vicinity of the reaction site. In platforms with an open droplet configuration (PT-based chips, Teflon-coated glass chips, and STT-based chips), the nitrogen flow could be eliminated, and it was also found that there was no need for azeotropic distillation steps, resulting in shorter synthesis time.<sup>28,31,32,53,54</sup> In addition, the evaporation was much faster in open-droplet platforms

**Table 1.** Summary of Droplet-Based Radiosynthesis Methods.

Droplet platform	EWOD (Generation 1)	EWOD (Generation 2)	Teflon-coated glass	Magnetic	Passive transport (PT)	Surface tension trap (STT)
Platform size	Very compact	Moderate	Very compact	Moderate	Compact	Compact
Chip size (mm <sup>2</sup> )	38 × 51	25 × 25	25 × 25	Not reported	25.0 × 27.5	25.0 × 27.5
Droplet configuration	Sandwiched	Sandwiched	Sandwiched or open	Open	Open	Open
Chip material	Glass with electrode layer, dielectric layer, and Teflon AF layer	Glass with electrode layer, dielectric layer, and Teflon AF layer	Glass with Teflon AF layer	Teflon sheet	Silicon with patterned Teflon AF layer	Silicon with patterned Teflon AF layer
Chip cost	High	High	Low	Very low	Low	Low
Droplet transport method	Sequential activation of buried electrodes	Sequential activation of buried electrodes	None	Magnetic particles in droplet follow a magnet moved below the substrate	Spontaneous movement along tapered hydrophilic channels	None
Reaction volume (μL)	1-16	10	0.15-8	100	2.0	6.0-20
Heating method	On-chip electrodes	External heater	External heater	None	External heater	External heater
Automated steps	Droplet transport, mixing, heating	Reagent loading; droplet transport, mixing, heating; product collection	None	Droplet transport and mixing; solvent removal	Reagent loading; droplet transport, heating; product collection	Reagent loading; heating; product collection
Reagent loading method	(Manual) Pipetting at edge of chip on demand	Pumping from pre-loaded reservoirs in disposable cassette through inlet holes in cover chip	(Manual) Pipetting directly to reaction site on demand	(Manual) Pipetting at start of synthesis	Non-contact piezoelectric dispensing. Dedicated channel per reagent.	Non-contact piezoelectric dispensing. Rotary stage moves reaction site to desired dispenser.
Product collection method	(Manual) Cover removal and pipetting	Vacuum applied to cassette draws liquid through outlet holes in cover chip	(Manual) Cover removal and pipetting	(Manual) Aspiration via syringe	Vacuum applied to dip tube lowered into the droplet	Vacuum applied to dip tube after droplet rotated into position
Additional Advantages	- Active mixing is possible - No moving parts	- Chip mounted in disposable cassette simplifies setup	- Easy to use - No moving parts	- Combines radioisotope concentration and synthesis in one platform - Solvent removal via capillary is faster than evaporation - Lack of heating limits applications - Drying method may be insufficient for water-sensitive reactions - Complicated preparation of magnetic particles	- Rapid heating, cooling and evaporation - Can perform limited radioisotope concentration on chip - Reagents not well confined to reaction zone - Low maximum volume	- Rapid heating, cooling, and evaporation - Can perform limited radioisotope concentration on chip
Limitations	- Defects in dielectric layer can lead to electrolysis - Closed structure has slower solvent evaporation than open structure	- Defects in dielectric layer can lead to electrolysis - Closed structure has slower solvent evaporation than open structure	- No steps are automated			

**Table 2.** Summary of Radiolabeled Molecules Synthesized Using Droplet-Based Radiosynthesis Platforms.<sup>a</sup>

Tracer	Assays	Droplet platform	Crude RCY (%)	Isolated RCY (%)	Reference
<sup>[18F]</sup> fallypride	D2/D3 receptor availability	EWOD (Generation 1)	82 ± 6 (n = 9)	65 ± 6 (n = 7)	40
		EWOD (Generation 1)	84 ± 7 (n = 6)	65 ± 11 (n = 6)	35
		PT	64 ± 6 (n = 4)	46 ± 4 (n = 4)	31
		EWOD (Generation 2)	40 ± 9 (n = 7)	Not reported	39
		STT	96 ± 3 (n = 9)	78 ± 1 (n = 1)	32
<sup>[18F]</sup> FDG	Glucose metabolism	EWOD (Generation 1)	32 ± 15 (n = 11)	22 ± 8 (n = 11)	38
		EWOD (Generation 1)	72 ± 13 (n = 5)	Not reported	51
		EWOD (Generation 1)	45 ± 10 (n = 2)	37 ± 13 (n = 2)	35
		EWOD (Generation 2)	50 ± 1 (n = 2)	Not reported	39
		Teflon-glass	Not reported	71 (n = 5) <sup>b</sup>	42
		PT	50 ± 8 (n = 4)	36 ± 6 (n = 4)	31
		EWOD (Generation 1)	74 ± 7 (n = 6)	56 ± 8 (n = 6)	35
<sup>[18F]</sup> FLT	Cell proliferation	EWOD (Generation 1)	69 ± 8 (n = 10)	63 ± 5 (n = 6)	41
		Teflon-glass	Not reported	71 (n = 5) <sup>b</sup>	43
<sup>[18F]</sup> SFB	(Prosthetic group)	EWOD (Generation 1)	34 ± 10 (n = 3)	19 ± 8 (n = 5)	35
		EWOD (Generation 1)	Not reported	39 ± 7 (n = 4)	52
<sup>[18F]</sup> FET	Amino acid transport	STT	59 ± 7 (n = 4)	55 ± 7 (n = 4)	53
		PT	54 ± 6 (n = 5)	Not reported	53
<sup>[18F]</sup> FDOPA	Dopaminergic function	STT	15 ± 2 (n = 4)	10 ± 1 (n = 4)	54
<sup>[18F]</sup> FBB	β-amyloid deposits	STT	70 ± 7 (n = 2)	Not reported	55
<sup>[18F]</sup> AMBF <sub>3</sub> -TATE	STTR2 expression	Teflon-glass	17 ± 3 (n = 15)	16 ± 1 (n = 5)	28
3-formyl-2,4,6-trimethylbenzene-sulfonyl <sup>[18F]</sup> fluoride	Prosthetic group	MDM	Not reported	72 ± 1 (n = 3)	36

<sup>a</sup>Crude RCY is the radiochemical conversion (measured by radio-TLC or radio-HPLC) multiplied by the fraction of initial activity that is collected from the chip, corrected for decay. Isolated RCY is the activity of isolated product divided by the initial activity, corrected for decay. Studies that reported only radiochemical conversion have been omitted.

<sup>b</sup>indicates that standard deviation is not reported in the related reference.

versus covered droplet platforms. Next, a precursor droplet was loaded to dissolve the dried residue of the dried <sup>[18F]</sup>fluoride complex and the chip was heated to perform the fluorination step. In EWOD chips, mixing was achieved by actuation of the reaction droplet in different directions prior to heating. For Teflon-coated glass chips, mixing was sometimes performed manually using a pipette to “stir” the reaction droplet. Mixing in other platforms (PT-based chip, STT-based chip) simply relied on convection and diffusion when a new droplet reached the reaction zone. Additional reaction steps (if needed) were performed in a similar fashion. Lastly, the crude product was collected from the chip by first adding droplets of a collection solution to solubilize the crude product and slightly increase the volume (to reduce fluid transfer losses), and then removing the larger resulting droplet (typically 10–20 μL). Often the collection process was repeated multiple (2–4) times to ensure high product recovery. For Teflon-glass chips and EWOD chips, collection was performed manually via pipette after separating the chips. For the second-generation EWOD platform in which the cover plate contained inlet and outlet ports, the diluted crude product droplet was collected by applying vacuum to the product output port. For the PT- and STT-based chips, the crude product was automatically transferred to the collection vial via vacuum by lowering the metal tubing or aligning the tubing with the reaction site, respectively.

Looking at <sup>[18F]</sup>fallypride as an example, there were some differences in synthesis performance among the various platforms. Crude radiochemical yield (crude RCY) using the first-generation EWOD platform was reported in 2 separate studies to be 82 ± 6% (n = 9)<sup>40</sup> and 84 ± 7% (n = 6).<sup>35</sup> Using the second-generation EWOD platform, the crude RCY was 40 ± 9% (n = 7).<sup>39</sup> While automation often results in slight reductions in performance due to residual liquid left in tubing and other fluid paths, such a large difference in yield in this instance is likely due to the fact that no optimization of conditions was performed for the second-generation platform. Using the PT platform, crude RCY was 64 ± 6% (n = 4),<sup>31</sup> while on the STT platform, it was improved to 96 ± 3% (n = 9)<sup>32</sup> by avoiding the problem of the reaction droplet spreading along the reagent delivery channels, which adversely affects mixing, fluorination conversion, and collection efficiency. An advantage of the STT and PT platforms was the open droplet configuration, which resulted in a shorter time for <sup>[18F]</sup>fluoride drying and an overall shorter synthesis, compared to the covered configuration of the EWOD chips.

Labeling of molecules with fluorine-18 via isotopic exchange (IEX) was also demonstrated on Teflon-coated glass chips, to produce <sup>[18F]</sup>AMBF<sub>3</sub>-TATE<sup>28</sup> and several o-trifluoroborato-phenylphosphonium compounds.<sup>56</sup> These 1-step syntheses were performed in a similar fashion to



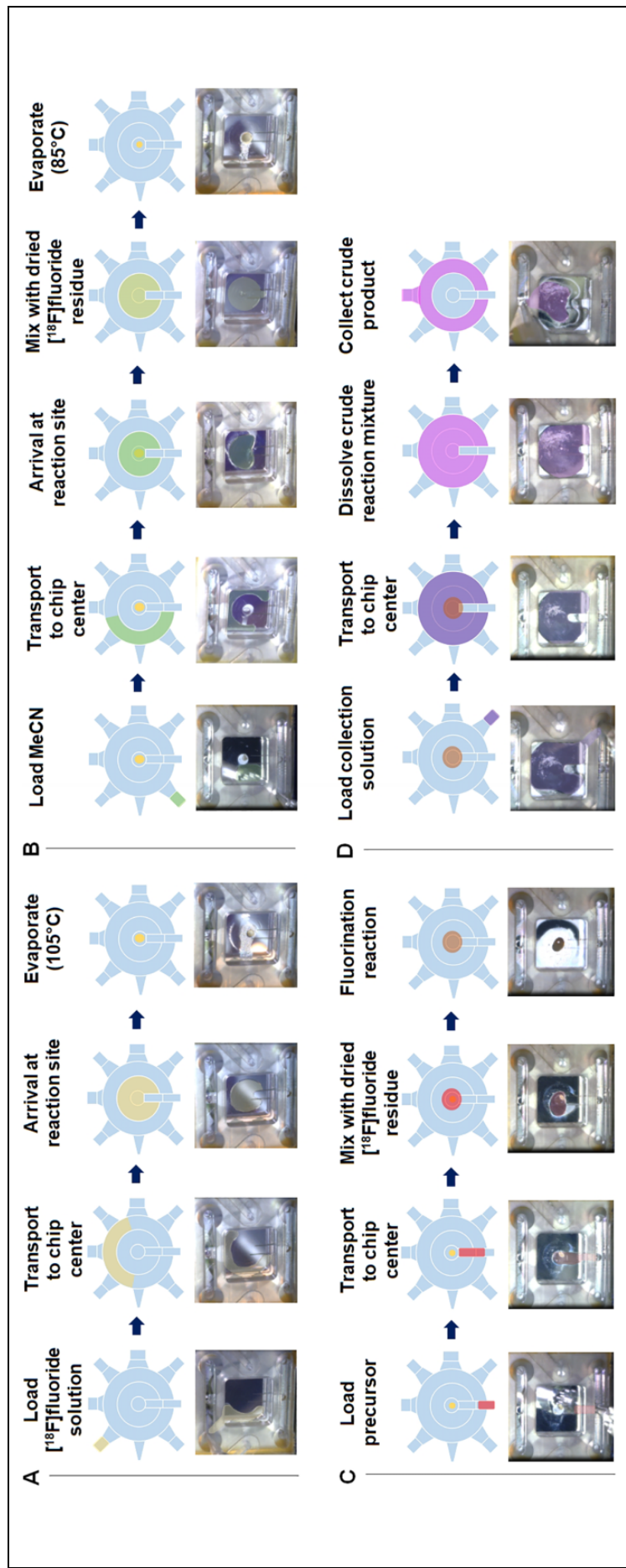


**Figure 2.** Schematic and representative micrographs of generic synthesis process for  $^{18}\text{F}$ -labeled tracers using the second-generation EWOD system. A, Steps involved in loading and drying of  $[^{18}\text{F}]$ fluoride solution. B, Steps involved in loading and evaporation of acetonitrile for removal of residual water via azeotropic drying to leave a dry, activated  $[^{18}\text{F}]$ fluoride residue. C, Steps involved in loading of precursor and performing radiofluorination reaction at elevated temperature. After the fluorination step, some tracers require loading of hydrolysis solution and reaction at elevated temperature to remove protecting groups (not shown). D, Steps involved in loading of collection solution to dissolve the crude product in a larger volume of solvent to facilitate efficient collection from the chip via vacuum with minimal residual liquid loss. The collected crude product then undergoes purification and formulation.

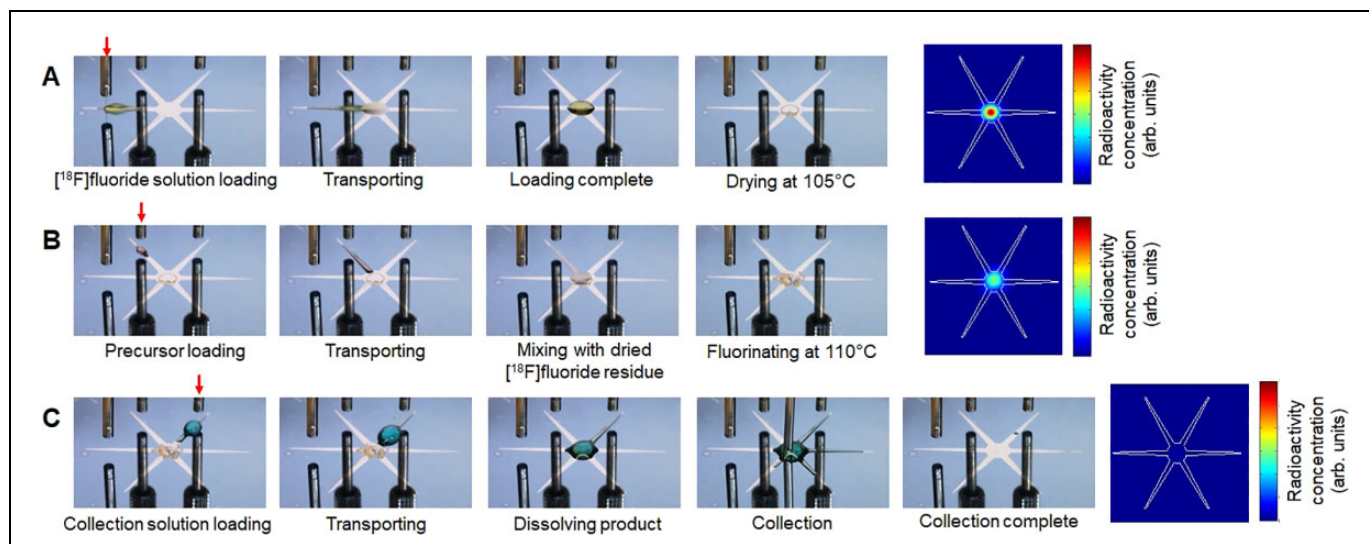


**Figure 3.** Operation of the passive-transport-based chip for a generic  $^{18}\text{F}$ -radiosynthesis. A, A  $^{18}\text{F}$ fluoride and phase transfer catalyst droplet (2  $\mu\text{L}$ ; dyed yellow) was loaded, spontaneously transported to the reaction site, and then the chip was heated to remove the solvent. B, Next, 2 droplets of the solvent mixture (1  $\mu\text{L}$ , dyed red) were loaded from a separate inlet and transported to the reaction site in sequence, after which the droplet was heated to perform the fluorination reaction. Note that loading in 2 separate portions instead of a single larger droplet helped to prevent over-flowing of the reaction site. C, Next, 2 droplets of collection solution (5  $\mu\text{L}$  each, dyed blue) were loaded from a third inlet and transported to the center to dilute the reaction mixture. Finally, the collection tubing was lowered and the droplet was collected into a vial with the aid of vacuum. Very little residue was apparent on the chip after collection. Red arrows indicate which dispenser is active during liquid loading steps. Images at the right of each row are Cerenkov images showing the distribution of activity on the chip after performing the steps depicted in each row. The boundary of the hydrophilic region is outlined in white. Adapted from Wang et al.<sup>31</sup> with permission from The Royal Society of Chemistry.

the process described above. A droplet of  $^{18}\text{F}$ fluoride and NaCl was first introduced and heated to remove the solvent, then a droplet of the buffered precursor solution was added and, finally, the chip was heated to perform the labeling reaction.

The procedure for synthesizing a sulfonyl  $^{18}\text{F}$ fluoride compound on the MDM platform (Figure 5) was significantly different from the above examples. Droplets of the initial  $^{18}\text{F}$ fluoride/ $^{18}\text{O}$ H<sub>2</sub>O solution were magnetically shuttled to a capillary tube to remove the  $^{18}\text{O}$ H<sub>2</sub>O, while leaving the  $^{18}\text{F}$ fluoride trapped on the QMA-derivatized magnetic particles. Prior to aspirating the liquid with the capillary, the magnetic particles were moved in a stirring motion within the droplet to ensure high trapping efficiency. After removing the aqueous solution, the particles (with trapped  $^{18}\text{F}$ fluoride) were mixed into a droplet containing K<sub>2</sub>CO<sub>3</sub> and precursor to release  $^{18}\text{F}$ fluoride in the solution and simultaneously perform the fluorination step at room temperature. The final product was then manually collected from the chip via syringe. The mechanism of  $^{18}\text{F}$ fluoride trapping and release using QMA-functionalized magnetic beads is quite interesting for this synthesis, though the degree of water removal and possible effects of beads present during the fluorination reaction need to be assessed to determine applicability of this platform to other  $^{18}\text{F}$ -radiosyntheses.

After the crude products of the abovementioned tracers were collected from the platforms, purification was performed using analytical-scale radio-HPLC, commercial solid phase

extraction (SPE) cartridges or customized miniature SPE cartridges. HPLC is in general a very versatile approach and can be used to achieve good separation of product for both labeled and non-labeled impurities, and was used after the droplet-based radiosyntheses of  $^{18}\text{F}$ Fallypride,  $^{18}\text{F}$ FET,  $^{18}\text{F}$ SFB,  $^{18}\text{F}$ FDOPA.<sup>31,32,40,53,54,52</sup> The small mass present in droplet-scale reactions allows the use of an analytical column instead of the semi-preparative column typically used in macroscale syntheses, and the narrow peak width allow very short retention times and thus short purification times. The volume of the collected fraction is generally very small (in the range  $\sim 1$ -2 mL), enabling rapid formulation of the purified product into an injectable solution either by dilution, or by evaporation of mobile phase followed by reconstitution in saline. Despite the success using HPLC, the large size and high cost of HPLC systems undermines many of the advantages that droplet radiochemistry provides.

In contrast, SPE is a straightforward purification method that can be implemented in a very compact space. SPE can be used for some radiopharmaceuticals, when the product structure is sufficiently distinct from reactants and impurities (or when the product is chemically-identical to the reactant, i.e. IEX reactions, and cannot be separated). Crude sulfonyl  $^{18}\text{F}$ fluoride from the MDM platform was purified using a commercial cartridge (Waters tC18 Light, 145 mg),<sup>36</sup> as was  $^{18}\text{F}$ AMBF<sub>3</sub>-TATE produced on the Teflon-coated glass chip (Waters C18 Plus, 360 mg).<sup>28</sup> A miniature cartridge was

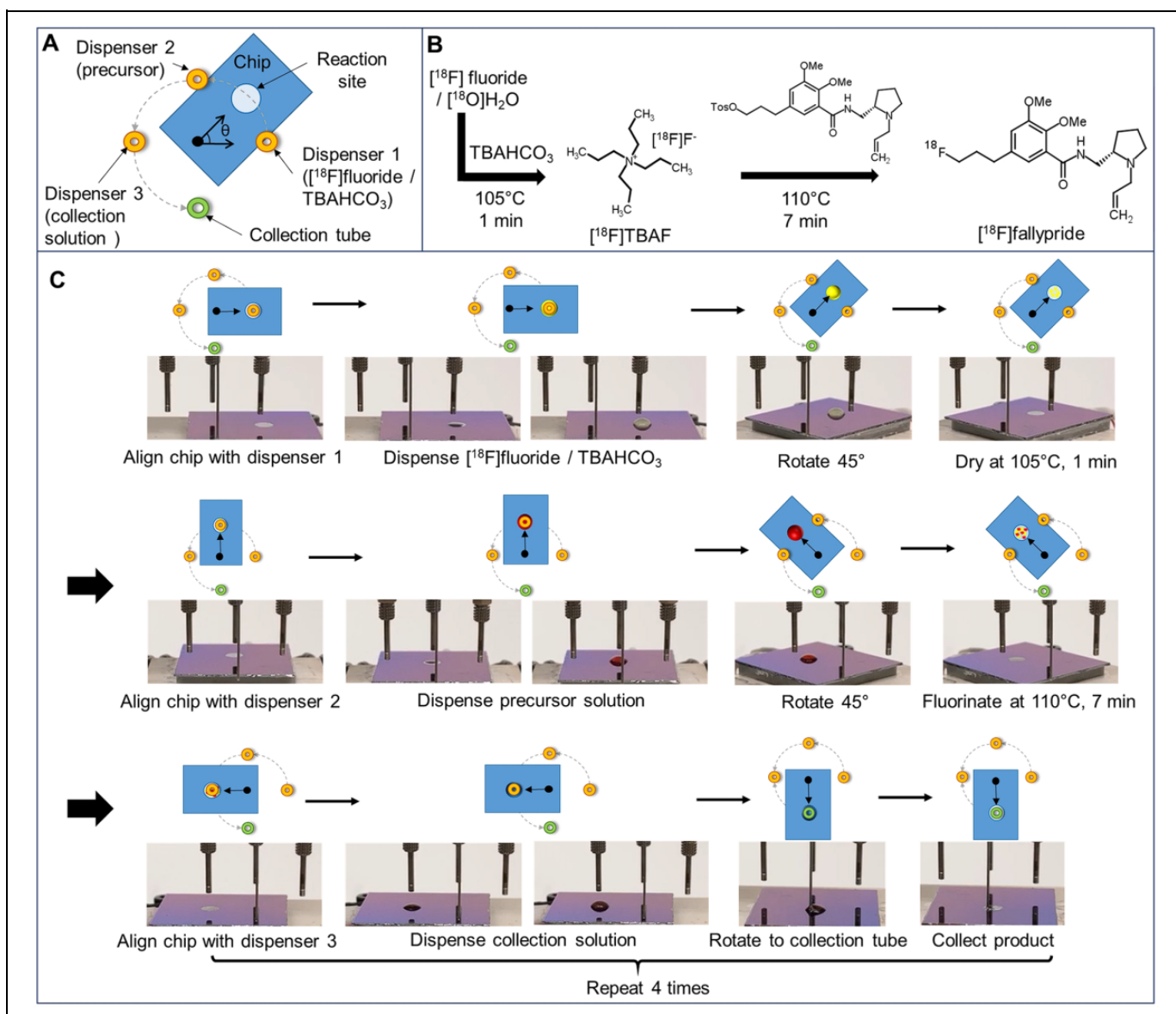


**Figure 4.** Operation of the surface-tension trap chip to perform the 1-step synthesis of  $[^{18}\text{F}]$ Fallypride. A, Top view schematic of the (moveable) microfluidic chip and (fixed) locations of reagent dispensers and the collection tube. The angle marker shows the center of rotation. B, Synthesis scheme. C, Schematic (showing chip orientation) and photograph of the chip for each step of the synthesis process. First the chip was rotated under the  $[^{18}\text{F}]$ fluoride mixture dispenser and 10 droplets (1  $\mu\text{L}$  each; dyed yellow) were loaded at the reaction site. Then, the chip was rotated slightly and heated to remove the solvent. Next, the chip was aligned under the precursor dispenser, 10 droplets (1  $\mu\text{L}$  each; dyed red) were loaded, and then the chip was heated to perform the fluorination reaction. Next, the chip was aligned under the collection solution dispenser and 20 droplets (1  $\mu\text{L}$ , dyed blue) were loaded to dilute the reaction mixture. Finally, the chip was rotated under the collection tube, and the droplet was collected into a product vial using vacuum. This whole collection process was repeated a total of 4 times to minimize the residual product left at the reaction site. Reproduced from Wang et al.<sup>32</sup> with permission from The Royal Society of Chemistry.

developed for purification of  $[^{18}\text{F}]$ FLT produced on the EWOD chip, consisting of multiple resins ( $\sim 180$  mg total) packed in a 1 ml syringe barrel.<sup>41</sup> Custom miniature cartridges were also used for purification of  $[^{18}\text{F}]$ FDG produced on the EWOD and PT platforms, and consisted of 4 different resins ( $\sim 60$  mg for EWOD,  $\sim 83$  mg for PT) packed into a length of tubing.<sup>31,38</sup> Purified probes were recovered from SPE cartridges in volumes ranging from 0.25 to 1.0 mL and then formulated. In general, the miniature cartridges reduced the volume of

solvents (and time needed) for trapping and rinsing, and also reduced the final eluted volume, compared to macroscale versions of the same SPE protocols.

### Reagent Economy and Time Efficiency

Performance of droplet-based radiosynthesizers is compared to that of conventional radiosynthesizers for multiple radiotracers in Table 3. Overall, the yield of tracers synthesized on the

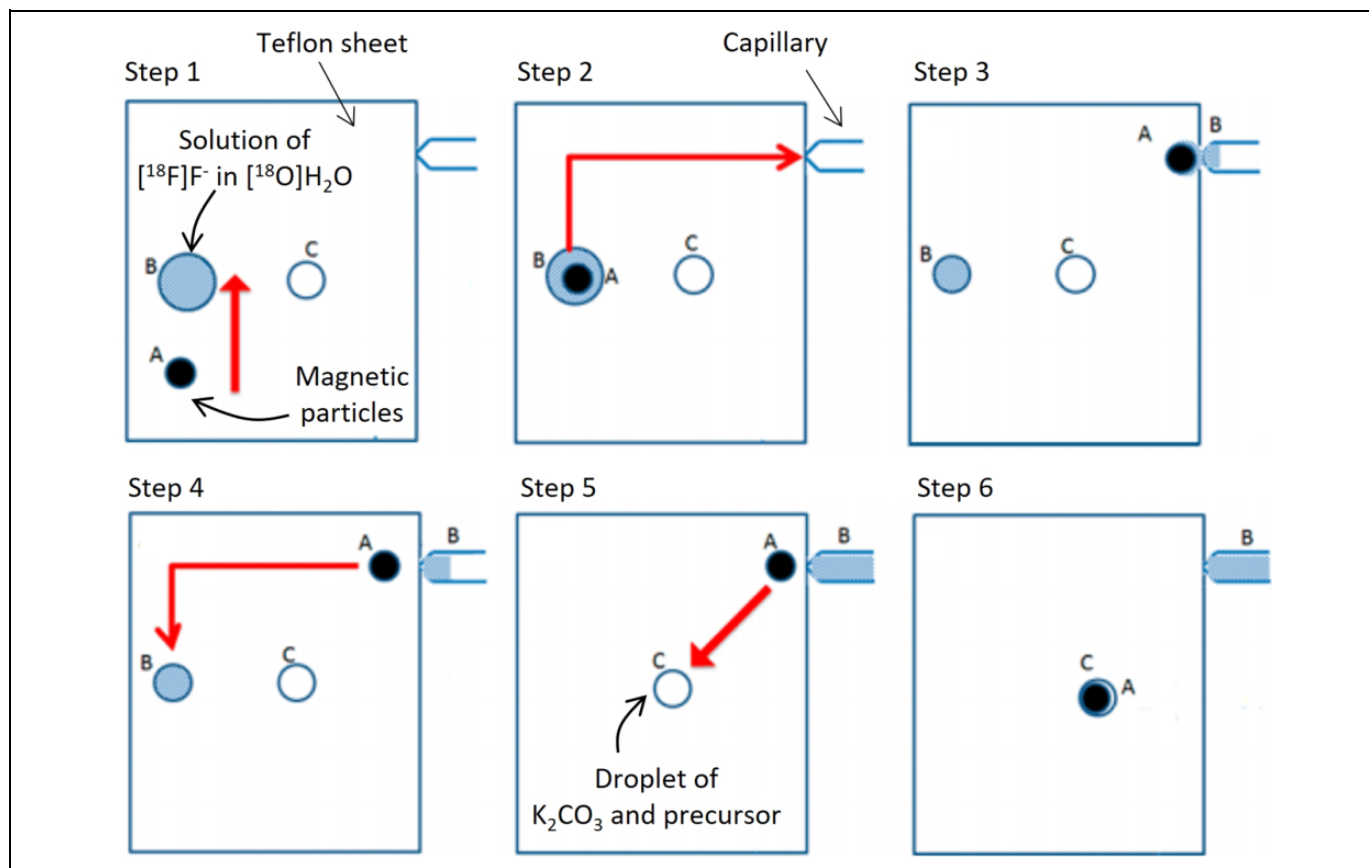


**Figure 5.** Steps for synthesis of a sulfonyl [ $^{18}\text{F}$ ]fluoride on the MDM platform. (Step 1) The magnetic particles (A) were moved toward the solution of [ $^{18}\text{O}$ ]H $_2\text{O}$  containing [ $^{18}\text{F}$ ]F $^-$ . The particles were looped in a circular stirring motion within the solution. (Step 2) The particles, carrying a portion of the solution as a droplet ( $\sim 50\ \mu\text{L}$ ), were then moved toward the capillary tube. (Step 3) The [ $^{18}\text{O}$ ]H $_2\text{O}$  was collected by the capillary tube under suction using a syringe pump, leaving [ $^{18}\text{F}$ ]F $^-$  bound to the QMA-functionalized magnetic beads. (Step 4) The particles were moved back to the [ $^{18}\text{F}$ ]F $^-$  / [ $^{18}\text{O}$ ]H $_2\text{O}$  solution to increase the activity trapped on the beads. Steps 2–4 were repeated continuously until the [ $^{18}\text{F}$ ]F $^-$  / [ $^{18}\text{O}$ ]H $_2\text{O}$  was completely consumed. (Step 5) The particles were then moved toward the mixed K $_2\text{CO}_3$  and precursor solution (C;  $\sim 100\ \mu\text{L}$ ) to release [ $^{18}\text{F}$ ]F $^-$  ions from the magnetic particles and perform the fluorination reaction. The particles were again looped in a circular motion within the solution to induce stirring. (6) The crude product was collected via syringe for downstream purification and formulation. Adapted from Fiel et al.<sup>36</sup> with permission from American Chemical Society, Copyright © 2015.

droplet-based platforms was comparable or even higher than on the conventional radiosynthesizers with much less reagents and shorter synthesis time.

One of the most noticeable features of droplet-based radiosynthesizers is reagent economy: in all cases (other than sulfonyl [ $^{18}\text{F}$ ]fluoride prepared via the MDM platform), the reactions required 1–2 orders of magnitude less precursor amount compared to the conventional radiosynthesizers. The small reaction volume of droplet reactions (2–10  $\mu\text{L}$ ) compared to conventional reaction (400–2000  $\mu\text{L}$ ) enabled the precursor concentration to be preserved (or even increased) during the microscale reaction, while reducing the total amount of precursor used in the reaction.

Another measure of efficiency is the synthesis time. The most recent droplet platforms have focused on streamlining processes to minimize the overall synthesis time. In particular, automated production of tracers on the PT- and STT-based reactors was completed in about half the time needed for the same synthesis on conventional platforms, leading to a

comparative advantage in activity yield. There are many contributing factors to the short synthesis times observed. The low reaction volume translates to low heat capacity, facilitating rapid heating and cooling of the reaction droplet during the synthesis. Evaporation steps are also greatly accelerated due to the much smaller volume of solvent to be removed. Furthermore, with  $< 100\ \mu\text{L}$  crude product collected from droplet-based radiosynthesizers and small mass amounts, the purification could be performed using analytical-scale radio-HPLC in  $< 10$  mins.<sup>31,32,53,54</sup> For conventional radiosynthesizers, a longer purification time was required due to the need to use semi-preparative scale radio-HPLC (typical retention times 10–30 min). Another advantage of analytical-scale HPLC is that the pure fraction is typically collected in a significantly smaller volume (e.g.  $\sim 1$ –2 mL compared to 10 s of mL), enabling faster downstream formulation. For tracers that were purified via SPE, synthesis time reductions were also observed because (i) there is less crude product volume that needs to be diluted and trapped on the SPE cartridge, (ii) miniature, low-

**Table 3.** Performance Comparison of Droplet-Based Radiosyntheses With Representative Results Using Conventional Automated Radiosynthesis Modules.<sup>a</sup>

Tracer	Format	Synthesis module	Automation	Reaction volume (μL)	Precursor amount (nmol)	Starting activity (GBq)	Synthesis time (min)	Activity yield (%)	Molar activity (GBq/μmol, at EOS)	Reference
<sup>18</sup> F]allylpride	Droplet	PT-based chip	Full	2	154	0.04	33	33 (n = 1)	185	31
	Droplet	STT-based chip	Full	6	231	0.02	30	65 (n = 1)	NR	32
	Conventional	TracerLab FX <sub>FN</sub> (GE)	Full	1000	3872	8.1-52	51 ± 1 (n = 42)	49 ± 1 (n = 42)	140-192	57
<sup>18</sup> F]FDG	Droplet	PT-based chip	Full	2	104	0.01	32	29 ± 5 (n = 4)	NR	31
	Conventional	ELIXYS FLEX/CHEM (Sofie)	Full	700	41300	3.7	38	55 ± 7 (n = 3)	NR	58
<sup>18</sup> F]FET	Droplet	STT-based chip	Manual <sup>b</sup>	10	60	0.4 ± 0.1	40	43 ± 5 (n = 4)	56-140	53
	Conventional	GRP (Scintomics)	Full	2000	15000	37-148	55	25 ± 5 (n = 20)	15-74	59
<sup>18</sup> F]FDOPA	Droplet	STT-based chip	Full	10	120	0.4	30	3.9 ± 1.8 (n = 3)	>370	54
	Conventional	ELIXYS FLEX/CHEM (Sofie)	Full	1000	16800	15	71	2.9 ± 0.8 (n = 3)	30-33	60
<sup>18</sup> F]SFB	Droplet	EWOD chip	Semi	2	168	0.2	120	18 ± 3 (n = 4)	NR	52
	Conventional	ELIXYS FLEX/CHEM (Sofie)	Full	1000	14000	3.7	88	40 ± 5 (n = 6)	63	61
<sup>18</sup> F]FLT	Droplet	EWOD chip	Semi	2	181	0.3	63	42 ± 3 (n = 5)	1800-2400	41
	Conventional	ELIXYS FLEX/CHEM (Sofie)	Full	1000	36000	3.7	85	38 ± 2 (n = 5)	67-481	61
<sup>18</sup> F]AMBF <sub>3</sub> -TATE	Droplet	Teflon-glass chip	Manual	5	5	0.93-1.1	35-45	12 ± 1 (n = 5)	29-144	28
	Conventional	AllInOne (Trasis)	Full	394	200	~150 <sup>c</sup>	60	10 ± 3 (n = 3)	440 ± 160 (n = 3)	62
3-formyl-2,4,6-trimethylbenzene-sulfonyl [ <sup>18</sup> F]fluoride	Droplet	MDM platform	Semi	60	3600	0.074-0.222	10-15	65 ± 1 (n = 3)	48 ± 3 (n = 3)	36
	Conventional	Conical vial	Manual	100	6000	0.185-0.37	27-31	73 ± 7 (n = 6)	105	63

<sup>a</sup>For conventional-scale comparisons, we selected literature reporting highest RCY and highest degree of automation. NR = not reported.

Notes:

<sup>b</sup>The synthesis can be automated, but results from manual syntheses are reported due to the more complete set of data reported.

<sup>c</sup>Estimated based on reported activity yield and RCY.

resin-mass cartridges could be washed with lower volumes of solvents, and (iii) miniature cartridges could be eluted with small volumes (which simplifies downstream formulation).

Other than shorter times needed for reaction, purification, and formulation, the volume reduction may also contribute to decreased overall synthesis time and complexity by eliminating process steps. For example, for reactions that require azeotropic drying steps after the initial [ $^{18}\text{F}$ ]fluoride drying step in conventional synthesis modules, it was found that these extra drying steps could be eliminated in open droplet platforms (PT and STT) for all tracers synthesized in those platforms.<sup>31,32,53,54</sup> In the case of [ $^{18}\text{F}$ ]FDOPA, the intermediate cartridge purification step needed after the fluorination step in the macroscale synthesis could be eliminated in the droplet-based synthesis,<sup>54,64,60</sup> shortening and simplifying the process, while achieving comparable RCY and radiochemical purity.

In addition to reduced precursor consumption as described above, the droplet-based synthesis format contributes to a greener process with reduced consumption of organic solvents and reduced production of waste. For example, solvents needed for crude [ $^{18}\text{F}$ ]FDOPA synthesis were reduced from 13 mL to 0.17 mL when moving from macroscale to the STT-based platform, and solvents consumed for purification were reduced from 65 mL to 9.3 mL due to the transition from semi-preparative to analytical-scale HPLC.<sup>54</sup> If the volumes of mobile phase consumed for column equilibration and cleaning were also factored in, 305 mL of HPLC mobile phase was consumed for the semi-preparative HPLC (macroscale synthesis) while only 57.3 mL were consumed for the analytical-scale system (microscale synthesis).

## High Molar Activity

During the production process of fluoride-18 labeled-tracers, the final product is always a mixture of  $^{18}\text{F}$ - and  $^{19}\text{F}$ -containing compounds due to unavoidable fluoride-19 contamination. Molar activity (or specific activity) is the ratio of quantity of  $^{18}\text{F}$ -labeled compounds to the total quantity of both  $^{18}\text{F}$ - and  $^{19}\text{F}$ -labeled compounds. Since only compounds labeled with the radioactive fluoride-18 can contribute the signal for PET scan, it is generally desirable that the injected radiotracer has high molar activity. It is important when the target of the tracer consists of saturable binding sites,<sup>65</sup> and is especially critical in preclinical imaging, where high concentrations of the tracer per mass of the animal is needed to achieve adequate signal-to-noise ratio.<sup>66</sup> For example, using droplet-based production of [ $^{18}\text{F}$ ]fallypride, we showed that molar activity (with constant amount of radioactivity injected) can have a drastic influence on the signal in the striata, with the contrast becoming progressively worse for lower molar activities<sup>44</sup> (Figure 6).

Interestingly, early work with EWOD chips showed that high molar activity was routinely achieved in droplet reactions, e.g. 730 GBq/ $\mu\text{mol}$  for [ $^{18}\text{F}$ ]fallypride (290 MBq starting activity),<sup>40</sup> and 1800-2400 GBq/ $\mu\text{mol}$  for [ $^{18}\text{F}$ ]FLT (330 MBq starting activity).<sup>41</sup> Our group performed a detailed study to understand the origin of this effect and how to optimize

synthesis for high molar activity.<sup>44</sup> In macroscale reactions, molar activity was found to increase linearly with starting activity (0.3-13.3 GBq), and vary inversely with reaction volume (0.1-3 mL; constant precursor concentration). However, in microscale reactions, molar activity was constant (and high) for all starting activities (0.9-19.4 GBq) and all volumes (2-8  $\mu\text{L}$ ). We concluded that reagents were the dominant source of [ $^{19}\text{F}$ ]fluoride contamination. Macroscale syntheses, with large reagents amounts, therefore only achieve high molar activity when using high starting activity (e.g. 10 s of GBq), consistent with general observations of synthesis performance in literature.<sup>67</sup> In contrast, the small quantity of reagents in microscale reactions introduces negligible [ $^{19}\text{F}$ ]fluoride contamination compared to the amount already present from the cyclotron and thus the molar activity of the final radiotracer is close to the molar activity of the fluoride source.

A consequence of this finding is that droplet-scale reactions are particularly well suited for making small batches (small activity level) of radiotracers such as needed for preclinical or in vitro studies.<sup>31,53,54</sup> For example, using the PT-based chips, high molar activity (185 GBq/ $\mu\text{mol}$ ) could be achieved starting with activity as low as 37 MBq.<sup>31</sup> With conventional methods, a large batch would need to be produced to ensure sufficient molar activity, but only a small amount of the batch would be used. Microscale reactions thus provide inherent safety and could be operated with much less shielding since the starting activities can be matched to the quantity of radiotracer actually needed.

The microliter-scale reaction volume can also be used to ensure high molar activity in isotopic exchange (IEX) reactions. There has been significant interest in several IEX reactions recently<sup>68</sup> due to the simple labeling process, mild conditions, and simple cartridge purification. In such reactions, the precursor and product are chemically identical and cannot be separated, so precursor amount needs to be minimized to maximize the molar activity. With conventional radiosynthesizers having 100 s of  $\mu\text{L}$  to mL reaction volumes, reported molar activities for IEX reactions are typically very low. Good molar activities can be achieved using techniques that allow smaller than usual reaction volumes in combination with high starting activities. For example, Liu et al. manually performed the synthesis of [ $^{18}\text{F}$ ]AMBF<sub>3</sub>-TATE in a volume of 120-150  $\mu\text{L}$  (containing 50 nmol of precursor) and achieved a molar activity of 110 GBq/ $\mu\text{mol}$  starting with 30-37 GBq of [ $^{18}\text{F}$ ]fluoride.<sup>69</sup> Lau et al. developed an automated synthesis with 400  $\mu\text{L}$  reaction (containing 200 nmol of precursor) and achieved molar activity of  $435 \pm 162$  GBq/ $\mu\text{mol}$  ( $n = 3$ ) with starting activity of  $\sim 150$  GBq.<sup>62</sup> Droplet radiochemistry techniques provide a way to dramatically reduce this reaction volume and precursor amount (and provide an automated way to do so). Using a Teflon-glass chip reactor, the reaction was performed in a 5  $\mu\text{L}$  reaction volume (5 nmol of precursor), and molar activity up to 144 GBq/ $\mu\text{mol}$  was observed with starting activities as low as 0.93-1.1 GBq.<sup>28</sup> Notably, the radiochemical yield was similar among all of these approaches. Microdroplet IEX approaches could likely be extended to other tracers based

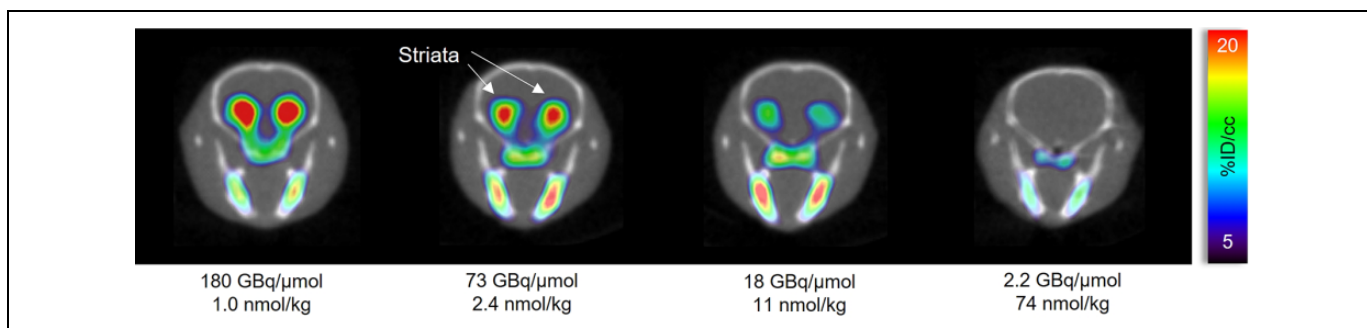


**Figure 6.** Effect of molar activity on [ $^{18}\text{F}$ ]fallypride PET/CT imaging in mice. Transverse projections of mouse brain from 10 min static scans after 60 min conscious uptake of [ $^{18}\text{F}$ ]fallypride. Molar activity values are reported at the time of injection, along with the total amount of fallypride injected per mass of the mouse. Adapted from Sergeev et al.<sup>44</sup> with permission from Springer Nature, Copyright © 2018.

on trifluoroborates,<sup>70,71</sup> aryl fluorosulfate<sup>72</sup> and silicon-fluoride<sup>73,74</sup> with the same benefits.

### Potential for Lower Cost Syntheses

Reduced consumption of starting materials by 1–2 orders of magnitude can reduce the synthesis cost substantially in the case of expensive or scarce precursors. The commercially-available precursors for many compounds can cost hundreds of USD for a single macroscale synthesis. The same amount of precursor can be used to perform a large number of droplet-scale reactions. For example, a total of 140 [ $^{18}\text{F}$ ]FDOPA syntheses (iodonium salt method) can be performed on the STT-based droplet reactor with the equivalent amount of precursor used in one single [ $^{18}\text{F}$ ]FDOPA synthesis on a conventional module.<sup>54</sup> Other than the benefit of lowering the cost, reduced need for precursors could also be a game-changer in the early stages of new tracer development when the precursor is very scarce. Instead of having only enough material to perform a few trial syntheses and then move quickly to *in vitro* or preclinical imaging studies, each macroscale-sized aliquot is sufficient to support a multitude of optimization experiments.

Simpler purification processes enabled by droplet-based radiosynthesizers can also have a significant impact. Shifting from semi-preparative scale to analytical scale HPLC, consumption of mobile phase is reduced more than 5x. In addition to the cost reduction, lower quantities of mobile phase reduce the environmental impact of radiopharmaceutical chemistry, consistent with widespread “green chemistry” efforts that are being made to reduce consumption and waste of toxic solvents in many areas of chemistry. Another impact of reducing column size is that analytical columns cost significantly less than semi-preparative columns, especially when their lifetime is factored in.

The shorter synthesis time provided by droplet-based radiosynthesizers reduces the cost of labor, and also frees up equipment earlier (radiosynthesizer and purification system), potentially allowing for the production of other tracers immediately afterward, maximizing the value of this equipment. To take advantage of this would require the development of a simple and safe chip-switching mechanism similar to the

cassette-based concept of some conventional-scale radiosynthesizers. Reduction in synthesis time also leads to improvement in activity yield. This can reduce the amount and cost of radioisotope needed for the synthesis, and the reduced amount of activity during the synthesis eases requirements for shielding (as further discussed below).

The ability to synthesize product with high molar activity, even with very little starting activity is a key advantage when only a small batch of the tracer is needed (e.g. for initial *in vitro* or *in vivo* evaluation studies). Whereas conventional methods would require the production of a large batch to achieve high molar activity, the microscale synthesis uniquely gives the possibility to make the tracers efficiently without wasting a large portion of the batch. In these cases, the small batch production can diminish the radionuclide cost for the tracer production. Working with lower radioactivity also has safety implications and may reduce the thickness of shielding needed.

Though some reports of droplet-based radiosynthesizers have operated the systems inside hot cells,<sup>36</sup> some were used behind an L-block in a standard fume hood.<sup>38,40,41</sup> In fact, due to the small size of droplet-based systems, in principle only a very small amount of shielding material would be needed to protect the operator from the gamma radiation. The STT platform was the first prototype with automated reagent delivery and product collection that was designed to minimize the overall system size,<sup>32</sup> and additional design iterations may result in even further size reductions. Already, the overall size of this microdroplet synthesis platform (including reagent loading, product collecting and temperature control) is an order of magnitude smaller than compact conventional radiosynthesizers on the market with similar functionality (e.g. Synthera+, IBA Radiopharma Solutions<sup>75</sup>). The droplet-radiochemistry instrument is also simpler than its conventional counterpart, potentially reducing the equipment cost component of each batch. Furthermore, the STT-based platform can potentially be self-shielded without requiring any specialized hot cells or mini cells.<sup>34</sup> These reduced needs can translate to significant cost reductions in radiopharmaceutical production, and can potentially open up new models for tracer production and distribution. For example, a new production facility could be set up with minimal space and capital, or an existing facility could be

upgraded with one more or more droplet synthesizers to increase capacity to produce multiple different tracers per day. Alternatively, compact, self-shielded, droplet radiosynthesizers could be directly installed in preclinical imaging centers or nuclear medicine clinics to increase flexibility of tracer production.

## Synthesis Scale-Up in the Droplet-Based Radiosynthesizers

Reports have shown that radiotracers produced via droplet-based methods have successfully been used for preclinical imaging, demonstrating sufficient quantity and concentration of each batch for multiple mouse or rat injections,<sup>28,31,38,44,53,76</sup> but, in general, activity scales are much lower than reports of macroscale syntheses (Table 3). If the final product activity could be scaled up in droplet-based radiosynthesizers, their applications could be further expanded to produce clinically-relevant amounts of radiopharmaceuticals.

Typically, droplet-based radiochemistry has been limited to 100 s of MBq of starting activity due to the  $\mu\text{L}$ -scale reaction volume compared to the radionuclide solution generated from cyclotron (about 1-5 mL), resulting in only a very small fraction of the initial activity loaded to the chip. To bridge the volume gap, several approaches were reported that could increase the production scale. Notably, in all approaches, the activity was scaled up while the amounts of other reagents were kept constant, consistent with typical approaches for scaling activity in conventional macroscale syntheses. Though we previously described some methods for concentrating [ $^{18}\text{F}$ ]fluoride in our previous review,<sup>34</sup> we provide here a comprehensive summary of the different approaches and results obtained by integrating them with droplet-based synthesizers.

In one technique demonstrated on EWOD chips, [ $^{18}\text{F}$ ]fluoride was concentrated by first loading and drying a large (200  $\mu\text{L}$ ) droplet of [ $^{18}\text{F}$ ]fluoride solution on the bottom substrate of the EWOD chip (in an open area of the chip immediately adjacent to the covered portion of the chip) until the volume was reduced to  $\sim 5 \mu\text{L}$ , and then the small droplet was pulled into the covered part of the chip by activating the electrodes sequentially.<sup>35</sup> These steps can be repeated to load an even greater amount of [ $^{18}\text{F}$ ]fluoride solution, but the 12 min time needed for concentration of each 200  $\mu\text{L}$  portion imposes some practical limits due to radioactive decay.

A different approach was demonstrated for activity concentration on the PT-based platform.<sup>31</sup> Instead of loading and drying a single large droplet of radioisotope solution, the volume was split into a series of 2  $\mu\text{L}$  droplets. Each small droplet of [ $^{18}\text{F}$ ]fluoride/[ $^{18}\text{O}$ ]H<sub>2</sub>O solution was dispensed at the reagent loading site, spontaneously transported to the pre-heated reaction site and dried upon arrival. After the final droplet of activity, a single droplet of phase transfer catalyst/base solution was added and dried. Though each small droplet can be dried in 10 s of seconds, significant scaling of this method requires a substantial amount of time.

The concentration method performed on the MDM platform follows a different strategy (Figure 5). QMA-functionalized magnetic beads were merged into a preloaded 1 mL drop of [ $^{18}\text{F}$ ]fluoride/[ $^{18}\text{O}$ ]H<sub>2</sub>O solution to trap [ $^{18}\text{F}$ ]fluoride. When the beads were magnetically actuated, they carried a portion of the volume ( $\sim 50 \mu\text{L}$ ) toward a small capillary, where the liquid ([ $^{18}\text{O}$ ]H<sub>2</sub>O) could be aspirated by applying vacuum. The steps were repeated multiple times to trap most of [ $^{18}\text{F}$ ]fluoride in the 1 mL solution. Trapping [ $^{18}\text{F}$ ]fluoride from an initial 1 mL volume of solution was reported to take only 5 min. The beads were then magnetically actuated to merge them with a 50  $\mu\text{L}$  droplet of aqueous K<sub>2</sub>CO<sub>3</sub> to release the [ $^{18}\text{F}$ ]fluoride from the beads into solution. This approach appears to work rapidly and efficiently to concentrate activity prior to aqueous reactions, but it is not clear if it can be adapted to water-sensitive fluorination reactions. Furthermore, the conditions optimized by the authors were limited to a trapping capacity of only  $\sim 100 \text{ MBq}$ , and further effort would be needed to explore whether that limit can be increased.

Recently, our group reported a standalone, automated concentrator system based on a miniaturized strong anion exchange (SAX) cartridge. The cartridge was prepared by packing 3 mg of Sep-Pak QMA resin inside tubing with miniature frits. The system could concentrate activity from 1 mL into a 12.4  $\mu\text{L}$  volume in 10 min, and had high efficiency for starting activities up to at least 37 GBq.<sup>77</sup> Larger volumes of radioisotope solution could be accommodated by extending the volume (and time) used in the trapping step. More recently, the concentrator was integrated with the PT-based radiosynthesizer to scale up the starting activity for the synthesis of [ $^{18}\text{F}$ ]Fallypride as shown in Figure 7.<sup>37</sup> An optimized method to transfer this volume to the chip was developed, consisting of delivery of the collected concentrated activity as a series of small (0.5  $\mu\text{L}$ ) droplets, followed by rinsing the activity collection vial and dispensing the rinse solution to the chip in the same fashion. Using this approach, 96% of the starting activity was loaded onto the chip and localized at the reaction site. Interestingly, as the synthesis of [ $^{18}\text{F}$ ]Fallypride was performed with increasing starting activity (4.5-41 GBq), the overall crude RCY of the synthesis in the 8  $\mu\text{L}$  volume began to drop, in part due to reduction of trapping efficiency of the miniaturized cartridges, and perhaps in part due to stoichiometric and/or radiolysis effects in the fluorination reaction at high activities. Even with this decreasing yield, a total of 7.2 GBq [ $^{18}\text{F}$ ]Fallypride product was produced in a single droplet reaction. The batches passed quality control tests suggesting the potential for clinically-relevant use in preparation of clinical doses or multi-dose batches (typical human dose is  $\sim 0.37 \text{ GBq}$ ). The overall time needed for concentration of the [ $^{18}\text{F}$ ]fluoride and transferring to the chip took only 17 min.

## Outlook

The last several years have brought significant new developments in droplet-based approaches for radiochemistry, using a variety of droplet manipulation techniques, to synthesize a



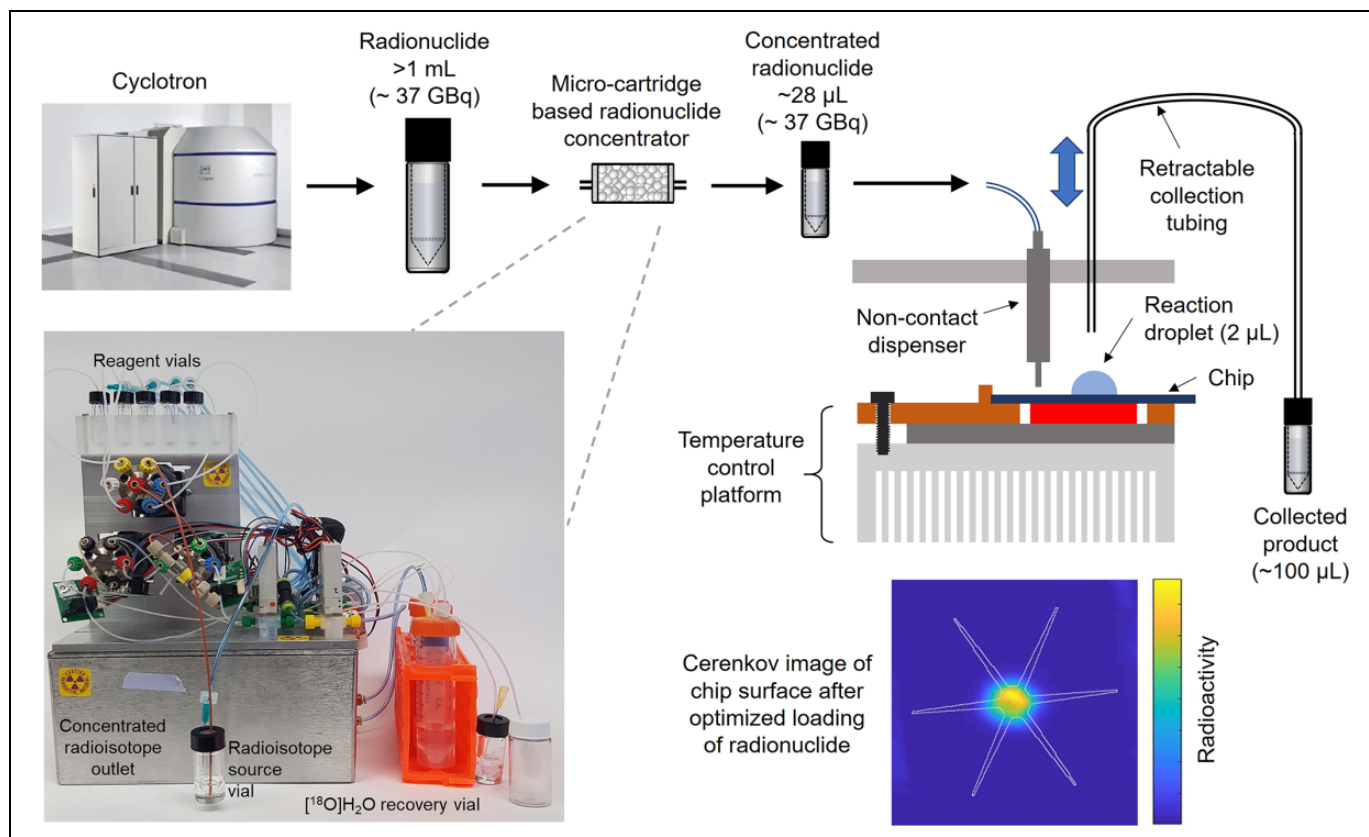


**Figure 7.** Schematic of the integrated system for high-activity droplet synthesis, including an automatic radionuclide concentrator subsystem (inset photograph) and a passive transport-based synthesis platform. The original radionuclide source (e.g. [ $^{18}\text{F}$ ]fluoride, >1 mL) is first concentrated to a small volume ( $\sim 28 \mu\text{L}$ ), and then dispensed to the chip as a series of small droplets and dried such that all of the radioactive residue is confined within the reaction zone of the chip (Cerenkov image inset at bottom right). The droplet-based synthesis is then carried out and the crude product collected, followed by downstream purification and formulation. Adapted from Wang et al.<sup>37</sup> with permission from The Royal Society of Chemistry.

diverse set of radiotracers. By many measures, droplet-based radiosynthesizers result in improved efficiency of tracer production, including lower cost, reduction of starting materials, greener synthesis process, shorter synthesis time, smaller system size, reduced need for shielding, and higher molar activity. These advantages could directly benefit production for a wide range of tracers explored so far (Table 2). In addition to these tracers reported in detail, the droplet-based reaction format has been used in pilot studies, including: (i) peptide labeling with [ $^{18}\text{F}$ ]FBEM,<sup>78</sup> (ii) peptide labeling with [ $^{18}\text{F}$ ]fluorobenzaldehyde, (iii) protein labeling with [ $^{18}\text{F}$ ]FBEM,<sup>78</sup> (iv) additional  $\text{BF}_3$  compounds labeled via isotopic exchange,<sup>56</sup> and (v) Ga-68 labeling of DOTA-containing peptides,<sup>79</sup> suggesting versatility for additional applications. Though we imagine applicability to a very wide variety of radiopharmaceuticals, the open structure of droplet-based chips does create a few limitations: reactions that involve gaseous reagents, and reaction conditions that generate high pressures (e.g. temperatures near or above solvent boiling points) will be difficult or impossible to implement. While operation of an EWOD chip inside a sealed pressurized chamber has been reported for hydrogenation reactions,<sup>80</sup> the setup may not be practical for radiochemistry applications.

As our lab and others continue to explore droplet radiochemistry, we expect there will be continued translation of known tracers from macroscale methods to droplet-based reactors, and eventually synthesis development could occur on the droplet platform itself to take advantage of the reagent economy and simple operation. The reduced consumption of reagents can enable  $\sim 2$  orders of magnitude more experiments to be performed (for synthesis optimization or production of batches for *in vitro* and *in vivo* studies) at early stages when the precursor is scarce. Toward the concept of optimization, our group recently developed a high-throughput chip that has multiple hydrophilic traps (Figure 8A) to perform up to 16 reactions simultaneously.<sup>81</sup> The reagent loading and product collection were performed manually on a temperature control module (Figure 8B), but a robotic system is under development to replace the manual intervention.<sup>82</sup> To enable analysis of the many samples produced using the high-throughput chip, we have recently shown the use of multi-lane radio-TLC separation and Cerenkov imaging for readout (Figure 8C, D).<sup>83</sup>

A niche application area of droplet-based radiosynthesizers is the efficient production of small batches (10 s of MBq) of tracers with high molar activity for research use, including *in*

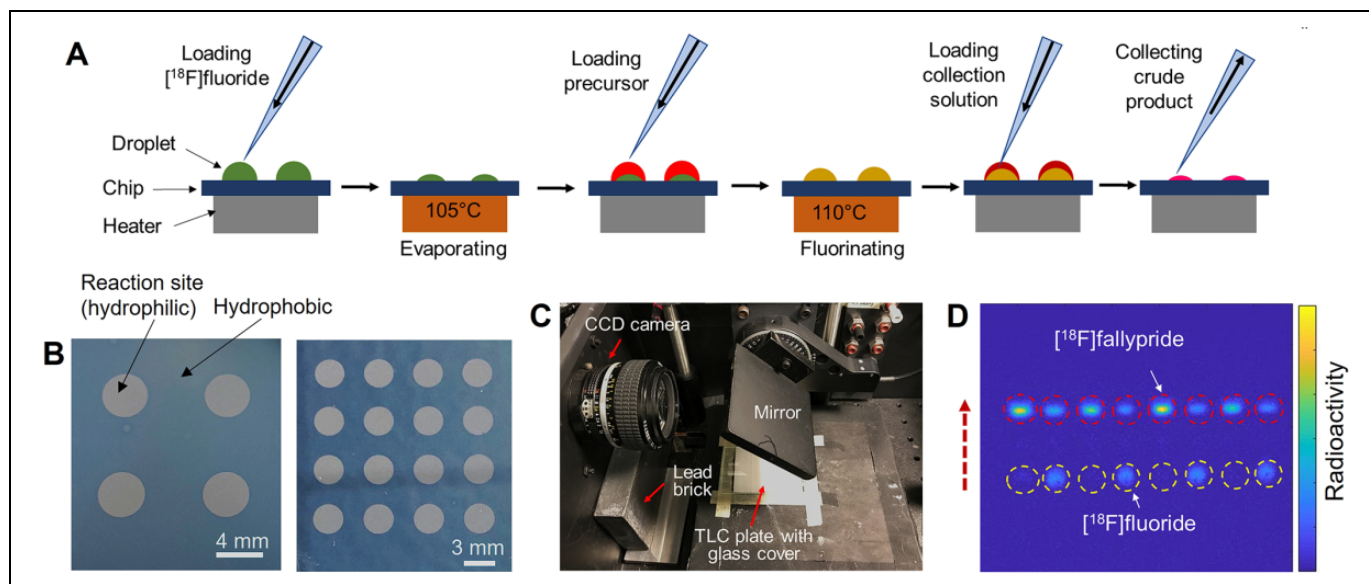


**Figure 8.** A, Schematic process to perform multiple simultaneous radiosynthesis using multi-reaction chips. B, Top view photographs of multi-reaction chips with 4 reaction sites (diameter 4 mm, pitch 9 mm) and 16 reaction sites (diameter 3 mm, pitch 5 mm). First, at each site, a droplet (8  $\mu\text{L}$ ) of [ $^{18}\text{F}$ ]fluoride mixed with phase transfer catalyst was added and then dried using heat. Then, a droplet of precursor solution (6  $\mu\text{L}$ ) was added and reacted at elevated temperature. Finally, 20  $\mu\text{L}$  of collection solution was loaded on the reaction site to dissolve resulting compounds and collected from the chip. Each site was collected for independent analysis via 3 repeats of the collection process. C, Photo of Cerenkov imaging setup for visualizing radioactivity distribution on multi-reaction chips or multi-lane radio-TLC plates. D, Cerenkov image of developed radio-TLC plate spotted with 8 droplets (0.5  $\mu\text{L}$ ) sampled from 8 different batches of crude [ $^{18}\text{F}$ ]fallypride reacted under different sets of conditions ( $n = 4$  replicates each of 2 different sets of conditions, spotted in alternating pattern). The dashed circles highlight the ROIs used for quantitative analysis of the 8 “lanes.” The dashed arrow represents the direction of solvent flow during developing. Parts A and B were adapted from Rios et al.<sup>81</sup> with permission from The Royal Society of Chemistry. Parts C and D were adapted from Wang et al.<sup>83</sup> with permission from Elsevier Inc., copyright © 2019. All rights reserved.

*vitro* studies for cell uptake, *in vivo* studies performed with preclinical imaging, and potentially single clinical doses. However, droplet radiosynthesis is not limited to only low-activity production. The possibility for synthesis at significant scale has also been demonstrated by using various radioisotope concentration strategies. In the case of [ $^{18}\text{F}$ ]Fallypride, production of >7 GBq of product was demonstrated. The observed reduction in yields at higher activity levels merit further study to determine the origins and find workarounds. These kinds of studies should be repeated to gather more data, and similar studies should be performed for other tracers to determine the range of production scale that is possible for each. The results of QC testing emphasized another important aspect of droplet-based radiochemistry: since the quantities of reagents and solvents are so low compared to macroscale methods, the tests all passed by very wide margins, providing enhanced safety. It is also possible to contemplate that it may be possible to streamline purification and/or QC testing processes by leveraging the intrinsically low amounts of impurities when the amount of precursor and other reagents is minimized.<sup>84</sup>

Both preclinical and clinical production in radiochemistry labs and radiopharmacies can greatly benefit from the space savings contributed by the compact size of droplet-radiosynthesis platforms. Taking up not much more spacing than a small coffee cup, multiple systems can be installed in existing hot cells to instantly increase capacity to produce

multiple tracers in a day, or potentially they can be operated in imaging labs or nuclear medicine clinics without the need for hot cells and just have compact, local shielding for operation. By installing new microscale systems, production of new tracers could be integrated into existing radiochemistry facilities without the need for additional hot cells or large radiosynthesis modules. Lowering the cost per batch could enable commercial supplies of tracers to be affordable for research purposes (which research dollars are spread thinly), and could remove bottlenecks inherent in centralized production and provide a much greater manufacturing capacity and thus produce less common tracers on a more frequent basis. Increased accessibility to various tracers could accelerate the development and validation of quantitative biological assays using these tracers, in addition to science that depends on the availability of such assays.

While the performance of the technologies, and capability for high-throughput studies, has significantly improved over the last several years, additional engineering is needed if such systems are to enter mainstream radiochemistry. (1) All of the fluidic components need to be integrated into a seamless, automated system to ensure safety, reliability and ease of use. We recently developed an automated radioactivity dispensing system that can be used to aliquot one batch of [ $^{18}\text{F}$ ]fluoride into portions for multiple droplet-based syntheses without manual intervention,<sup>85</sup> and we also are developing an automated

system to inject the crude product collected from the droplet-based radiosynthesizers into the radio-HPLC for purification. Development of more compact purification systems and integration with miniature formulation systems<sup>86</sup> are active areas of research. (2) It would be helpful to develop automated cleaning protocols to simplify operation and improve the lifetime of reagent dispensers, or alternatively, one could develop dispensing methods that do not require cleaning. (3) Especially for intended operation on the benchtop, a gas-tight enclosure will be needed to capture any release of radioactive vapor during the synthesis, and compact shielding for the synthesizer and purification system must be developed and validated. The gas-tight enclosure would likely also be preferred in clinical settings to help achieve aseptic conditions during the whole synthesis process. (4) A user-friendly software interface is needed to support performing established synthesis protocols, to facilitate programming of new protocols and to modify/optimize protocols. In the meantime, however, since manual and semi-automated syntheses are fully compatible with cGMP production, it would be interesting to explore the integration of a droplet synthesizer into a clinical production workflow.

Maybe the most significant obstacle to realizing the full potential of these systems is the lack of flexible and high-resolution purification methods that fit within an overall compact footprint. Due to the very small output volume and mass, most studies have switched from semi-preparative to analytical-scale HPLC for purification, reducing purification time, solvent consumption, and volume of the collected pure fraction (which can simplify formulation). But the column size reduction does not significantly reduce the overall size of the components that need to be shielded, nor cost of the purification system. From published papers,<sup>32,54</sup> the chromatograms are extremely clean, indicating not only the potential to further speed up the HPLC methods, but perhaps replace them with simpler and faster purification methods. Some of these were discussed in our previous review, including approaches for scavenging of unreacted [<sup>18</sup>F]fluoride by using alumina particles on the sandwiched chips,<sup>24,25</sup> and miniature resin-based solid-phase extraction cartridges implemented in microchannels or tubing.<sup>29,31,38,41</sup> Replacing resins with polymer monoliths could provide improved manufacturing and integration and provide a more stable physical geometry and flow properties.<sup>87</sup> While there have not been significant developments reported recently, these directions and other methods of separation continue to be actively pursued.

As a closing remark, we speculate that the droplet radio-synthesis technologies may also be extended to additional PET isotopes, SPECT isotopes, or therapeutic isotopes, providing a means to safely manufacture batches of these compounds on demand with very little need for space or upfront capital costs. Because most of these isotopes are also typically used in extremely low concentrations, the platform could provide comparable advantages for these other radiopharmaceuticals including convenient and compact means for preparation, reduction of precursor consumption, greener processes, and faster syntheses.

## Declaration of Conflicting Interests


The author(s) declared the following potential conflicts of interest with respect to the research, authorship, and/or publication of this article: The Regents of the University of California have licensed some of the described technology to Sofie, Inc. that was invented by Dr. van Dam, and have taken equity in Sofie, Inc. as part of the licensing transaction. Dr. van Dam is a founder of, and receives research support from, Sofie. Dr. Wang declares no conflict of interest.

## Funding

The author(s) disclosed receipt of the following financial support for the research, authorship, and/or publication of this article: We gratefully acknowledge support for writing this review from the National Cancer Institute (R33 CA240201) and the National Institute of Mental Health (R44 MH097271).

## ORCID iD

Jia Wang  <https://orcid.org/0000-0002-0070-1320>

R. Michael van Dam  <https://orcid.org/0000-0003-2316-0173>

## References

1. Phelps ME. Positron emission tomography provides molecular imaging of biological processes. *Proc Natl Acad Sci U S A*. 2000;97(16):9226–9233.
2. Hargreaves R. The role of molecular imaging in drug discovery and development. *Clin Pharmacol Ther*. 2008;83(2):349–353.
3. Glaudemans AWJM, de Vries EFJ, Galli F, Dierckx RA, Slart RH, Signore A. The use of 18F-FDG-PET/CT for diagnosis and treatment monitoring of inflammatory and infectious diseases. *Clin Dev Immunol*. 2013;2013:1–14.
4. Avril S, Muzic RF, Plecha D, Traughber BJ, Vinayak S, Avril N. 18F-FDG PET/CT for monitoring of treatment response in breast cancer. *J Nucl Med*. 2016;57(Suppl 1):34S–39S.
5. Kulkarni HR, Singh A, Langbein T, et al. Theranostics of prostate cancer: from molecular imaging to precision molecular radiotherapy targeting the prostate specific membrane antigen. *Br J Radiol*. 2018;91(1091):20180308.
6. Velikyan I. Molecular imaging and radiotherapy: theranostics for personalized patient management. *Theranostics*. 2012;2(5):424–426.
7. Rensch C, Jackson A, Lindner S, et al. Microfluidics: a ground-breaking technology for PET tracer production? *Molecules*. 2013;18(7):7930–7956.
8. Knapp K-A, Nickels ML, Manning HC. The current role of microfluidics in radiofluorination chemistry. *Mol Imaging Biol*. 2020;22(3):463–475.
9. Razzaq T, Kappe CO. Continuous flow organic synthesis under high-temperature/pressure conditions. *Chem Asian J*. 2010;5(6):1274–1289.
10. Wiles C, Watts P. Continuous flow reactors, a tool for the modern synthetic chemist. *Eur J Org Chem*. 2008;2008(10):1655–1671.
11. Arima V, Watts P, Pascali G. Microfluidics in planar microchannels: synthesis of chemical compounds on-chip. In: Castillo-León J, Svendsen WE, eds. *Lab-on-a-Chip Devices and Micro-Total*

- Analysis Systems*. Springer International Publishing; 2014: 197–239.
12. Pascali G, Watts P, Salvadori PA. Microfluidics in radiopharmaceutical chemistry. *Nucl Med Biol*. 2013;40(6):776–787.
  13. Zeng D, Desai AV, Ranganathan D, et al. Microfluidic radiolabeling of biomolecules with PET radiometals. *Nucl Med Biol*. 2013;40(1):42–51.
  14. Wright BD, Whittenberg J, Desai A, et al. Microfluidic preparation of a <sup>89</sup>Zr-labeled trastuzumab single-patient dose. *J Nucl Med*. 2016;57(5):747–752.
  15. Pfaff S, Philippe C, Pichler V, Hacker M, Mitterhauser M, Wadsak W. Microfluidic <sup>68</sup>Ga-labeling: a proof of principle study. *Dalton Trans*. 2018;47(17):5997–6004.
  16. Liu Z, Schaap KS, Ballemans L, et al. Measurement of reaction kinetics of [<sup>177</sup>Lu]Lu-DOTA-TATE using a microfluidic system. *Dalton Trans*. 2017;46(42):14669–14676.
  17. De Leonardi F, Pascali G, Salvadori PA, Watts P, Pamme N. On-chip pre-concentration and complexation of [<sup>18</sup>F]fluoride ions via regenerable anion exchange particles for radiochemical synthesis of positron emission tomography tracers. *J Chromatogr A*. 2011;1218(29):4714–4719.
  18. Sadeghi S, Liang V, Cheung S, et al. Reusable electrochemical cell for rapid separation of [<sup>18</sup>F]fluoride from [<sup>18</sup>O]water for flow-through synthesis of <sup>18</sup>F-labeled tracers. *Appl Radiat Isot*. 2013;75:85–94.
  19. Arima V, Pascali G, Lade O, et al. Radiochemistry on chip: towards dose-on-demand synthesis of PET radiopharmaceuticals. *Lab Chip*. 2013;13(12):2328–2336.
  20. Tarn MD, Pascali G, De Leonardi F, Watts P, Salvadori PA, Pamme N. Purification of 2-[<sup>18</sup>F]fluoro-2-deoxy-d-glucose by on-chip solid-phase extraction. *J Chromatogr A*. 2013;1280:117–121.
  21. Saiki H, Iwata R, Nakanishi H, et al. Electrochemical concentration of no-carrier-added [<sup>18</sup>F]fluoride from [<sup>18</sup>O]water in a disposable microfluidic cell for radiosynthesis of <sup>18</sup>F-labeled radiopharmaceuticals. *Appl Radiat Isot*. 2010;68(9):1703–1708.
  22. Wong R, Iwata R, Saiki H, Furumoto S, Ishikawa Y, Ozeki E. Reactivity of electrochemically concentrated anhydrous [<sup>18</sup>F]fluoride for microfluidic radiosynthesis of <sup>18</sup>F-labeled compounds. *Appl Radiat Isot*. 2012;70(1):193–199.
  23. Lee C-C, Sui G, Elizarov A, et al. Multistep synthesis of a radiolabeled imaging probe using integrated microfluidics. *Science*. 2005;310(5755):1793–1796.
  24. Chen S, Lei J, van Dam RM, et al. Planar alumina purification of <sup>18</sup>F-labeled radiotracer synthesis on EWOD chip for positron emission tomography (PET). In: *Proceedings of the 16th International Conference on Miniaturized Systems for Chemistry and Life Sciences*; 2012:1771–1773.
  25. Chen S, Dooraghi A, Lazari M, et al. On-chip product purification for complete microfluidic radiotracer synthesis. In: *Proceedings of the 27th IEEE International Conference on Micro Electro Mechanical Systems (MEMS)*. San Francisco, CA. January 26–30, 2014:284–287.
  26. Zhang X, Liu F, Knapp K-A, Nickels ML, Manning HC, Bellan LM. A simple microfluidic platform for rapid and efficient production of the radiotracer [<sup>18</sup>F]fallypride. *Lab Chip*. 2018;18(9):1369–1377.
  27. Keng PY, Sergeev M, van Dam RM. Advantages of radiochemistry in microliter volumes. In: Kuge Y, Shiga T, Tamaki N, eds. *Perspectives on Nuclear Medicine for Molecular Diagnosis and Integrated Therapy*. Springer Japan; 2016:93–111.
  28. Lisova K, Sergeev M, Evans-Axelsson S, et al. Microscale radiosynthesis, preclinical imaging and dosimetry study of [<sup>18</sup>F]AMBF3-TATE: a potential PET tracer for clinical imaging of somatostatin receptors. *Nucl Med Biol*. 2018;61:36–44.
  29. Rensch C, Lindner S, Salvamoser R, et al. A solvent resistant lab-on-chip platform for radiochemistry applications. *Lab Chip*. 2014;14(14):2556–2564.
  30. Frank C, Winter G, Rensei F, et al. Development and implementation of ISAR, a new synthesis platform for radiopharmaceutical production. *EJNMMI Radiopharm Chem*. 2019;4(1):24.
  31. Wang J, Chao PH, Hanet S, van Dam RM. Performing multi-step chemical reactions in microliter-sized droplets by leveraging a simple passive transport mechanism. *Lab Chip*. 2017;17(24):4342–4355.
  32. Wang J, Chao PH, van Dam RM. Ultra-compact, automated microdroplet radiosynthesizer. *Lab Chip*. 2019;19(14):2415–2424.
  33. Iwata R, Pascali C, Terasaki K, et al. Practical microscale one-pot radiosynthesis of <sup>18</sup>F-labeled probes. *J Labelled Comp Radiopharm*. 2018;61(7):540–549.
  34. Keng PY, van Dam RM. Digital microfluidics: a new paradigm for radiochemistry. *Mol Imag*. 2015;14(12):579–594.
  35. Chen S, Javed MR, Kim H-K, et al. Radiolabelling diverse positron emission tomography (PET) tracers using a single digital microfluidic reactor chip. *Lab Chip*. 2014;14(5):902–910.
  36. Fiel SA, Yang H, Schaffer P, et al. Magnetic droplet microfluidics as a platform for the concentration of [<sup>18</sup>F]fluoride and radiosynthesis of sulfonyl [<sup>18</sup>F]fluoride. *ACS Appl Mater Interfaces*. 2015;7(23):12923–12929.
  37. Wang J, Chao PH, Slavik R, van Dam RM. Multi-GBq production of the radiotracer [<sup>18</sup>F]fallypride in a droplet microreactor. *RSC Adv*. 2020;10(13):7828–7838.
  38. Keng PY, Chen S, Ding H, et al. Micro-chemical synthesis of molecular probes on an electronic microfluidic device. *Proc Natl Acad Sci U S A*. 2012;109(3):690–695.
  39. Wang J. Radiochemistry in microdroplets: technologies and applications. Doctoral dissertation, University of California Los Angeles, Los Angeles, CA, USA. 2019.
  40. Javed MR, Chen S, Lei J, et al. High yield and high specific activity synthesis of [<sup>18</sup>F]fallypride in a batch microfluidic reactor for micro-PET imaging. *Chem Commun*. 2014;50(10):1192–1194.
  41. Javed MR, Chen S, Kim H-K, et al. Efficient radiosynthesis of 3'-deoxy-3'-<sup>18</sup>F-fluorothymidine using electrowetting-on-dielectric digital microfluidic chip. *J Nucl Med*. 2014;55(2):321–328.
  42. Koag MC, Kim H-K, Kim AS. Efficient microscale synthesis of [<sup>18</sup>F]-2-fluoro-2-deoxy-d-glucose. *Chem Eng J*. 2014;258:62–68.
  43. Koag MC, Kim H-K, Kim AS. Fast and efficient microscale radiosynthesis of 3'-deoxy-3'-[<sup>18</sup>F]fluorothymidine. *J Fluor Chem*. 2014;166:104–109.

44. Sergeev M, Lazari M, Morgia F, et al. Performing radiosynthesis in microvolumes to maximize molar activity of tracers for positron emission tomography. *Communi Chem*. 2018;1(1):10.
45. Li J, Ha NS, T 'Leo' Liu, van Dam RM, 'CJ' Kim CJ. Ionic-surfactant-mediated electro-dewetting for digital microfluidics. *Nature*. 2019;572(7770):507–510.
46. Park S-Y, Teitell MA, Chiou EPY. Single-sided continuous optoelectrowetting (SCOEW) for droplet manipulation with light patterns. *Lab Chip*. 2010;10(13):1655–1661.
47. Darhuber AA, Valentino JP, Troian SM. Planar digital nanoliter dispensing system based on thermocapillary actuation. *Lab Chip*. 2010;10(8):1061–1071.
48. Guttenberg Z, Müller H, Habermüller H, et al. Planar chip device for PCR and hybridization with surface acoustic wave pump. *Lab Chip*. 2005;5(3):308–317.
49. Zhang Y, Nguyen N-T. Magnetic digital microfluidics—a review. *Lab Chip*. 2017;17(6):994–1008.
50. Yu W, Lin H, Wang Y, et al. A ferrobotic system for automated microfluidic logistics. *Sci Robot*. 2020;5(39):eaba4411.
51. Dooraghi AA, Keng PY, Chen S, et al. Optimization of microfluidic PET tracer synthesis with Cerenkov imaging. *Analytst*. 2013;138(19):5654–5664.
52. Kim H-K, Rashed Javed M, Chen S, et al. On-demand radiosynthesis of N-succinimidyl-4-[18 F]fluorobenzoate ([18 F]SFB) on an electrowetting-on-dielectric microfluidic chip for 18 F-labeling of protein. *RSC Adv*. 2019;9(55):32175–32183.
53. Lisova K, Chen BY, Wang J, Fong KM, Clark PM, van Dam RM. Rapid, efficient, and economical synthesis of PET tracers in a droplet microreactor: application to O-(2-[18F]fluoroethyl)-L-tyrosine ([18F]FET). *EJNMMI Radiopharm Chem*. 2019;5(1):1.
54. Wang J, Holloway T, Lisova K, van Dam RM. Green and efficient synthesis of the radiopharmaceutical [18 F]FDOPA using a microdroplet reactor. *React Chem Eng*. 2020;5(2):320–329.
55. Lisova K, Wang J, Rios A, et al. Adaptation and optimization of [F-18] Flortbetaben ([F-18] FBB) radiosynthesis to a microdroplet reactor. *Journal of Labelled Compounds & Radiopharmaceuticals*; 2019:S353–S354.
56. Lisova K, Pla D, Sergeev, et al. Leveraging microvolume radiochemistry and trifluoroborate chemistry to synthesize 18F-labeled prosthetic groups via isotopic exchange with high specific activity. *Journal of Labelled Compounds and Radiopharmaceuticals*; 2017:S37.
57. Seok Moon B, Hyung Park J, Jin Lee H, et al. Highly efficient production of [18F]fallypride using small amounts of base concentration. *Appl Radiat Isot*. 2010;68(12):2279–2284.
58. Long JZ, Jacobson MS, Hung JC. Comparison of FASTlab 18F-FDG production using phosphate and citrate buffer cassettes. *J Nucl Med Technol*. 2013;41(1):32–34.
59. Siddiq IS, Atwa ST, Shama SA, et al. Radiosynthesis and modified quality control of O-(2-[18F]fluoroethyl)-L-tyrosine ([18F]FET) for brain tumor imaging. *Appl Radiat Isot*. 2018;133:38–44.
60. Collins J, Waldmann CM, Drake C, et al. Production of diverse PET probes with limited resources: 24 <sup>18</sup>F-labeled compounds prepared with a single radiosynthesizer. *Proc Natl Acad Sci U S A*. 2017;114(43):11309–11314.
61. Lazari M, Collins J, Shen B, et al. Fully automated production of diverse 18F-labeled PET tracers on the ELIXYS multireactor radiosynthesizer without hardware modification. *J Nucl Med Technol*. 2014;42(3):203–210.
62. Lau J, Pan J, Rousseau E, et al. Pharmacokinetics, radiation dosimetry, acute toxicity and automated synthesis of [18F]AmBF3-TATE. *EJNMMI Res*. 2020;10(1):25.
63. Inkster JAH, Liu K, Ait-Mohand S, et al. Sulfonyl fluoride-based prosthetic compounds as potential 18F labelling agents. *Chemistry*. 2012;18(35):11079–11087.
64. Kuik W-J, Kema IP, Brouwers AH, et al. In vivo biodistribution of no-carrier-added 6-18F-fluoro-3,4-dihydroxy-L-phenylalanine (18F-DOPA), produced by a new nucleophilic substitution approach, compared with carrier-added 18F-DOPA, prepared by conventional electrophilic substitution. *J Nucl Med*. 2015;56(1):106–112.
65. Kung M-P, Kung HF. Mass effect of injected dose in small rodent imaging by SPECT and PET. *Nucl Med Biol*. 2005;32(7):673–678.
66. Jagoda EM, Vaquero JJ, Seidel J, Green MV, Eckelman WC. Experiment assessment of mass effects in the rat: implications for small animal PET imaging. *Nucl Med Biol*. 2004;31(6):771–779.
67. Lapi SE, Welch MJ. A historical perspective on the specific activity of radiopharmaceuticals: what have we learned in the 35 years of the ISRC? *Nucl Med Biol*. 2013;40(3):314–320.
68. Bernard-Gauthier V, Bailey JJ, Liu Z, et al. From unorthodox to established: the current status of 18F-Trifluoroborate- and 18F-SiFA-based radiopharmaceuticals in PET nuclear imaging. *Bioconjug Chem*. 2016;27(2):267–279.
69. Liu Z, Pourghasian M, Bénard F, Pan J, Lin KS, Perrin DM. Preclinical evaluation of a high-affinity 18F-trifluoroborate octreotate derivative for somatostatin receptor imaging. *J Nucl Med*. 2014;55(9):1499–1505.
70. Kuo H-T, Lepage M, Lin K-S, et al. One-step 18F-labeling and preclinical evaluation of prostate specific membrane antigen trifluoroborate probes for cancer imaging. *J Nucl Med*. 2019;60(8):1160–1166.
71. Roxin Á, Zhang C, Huh S, et al. A metal-free DOTA-conjugated 18F-labeled radiotracer: [18F]DOTA-AMBF3-LLP2A for imaging VLA-4 over-expression in murine melanoma with improved tumor uptake and greatly enhanced renal clearance. *Bioconjug Chem*. 2019;30(4):1210–1219.
72. Zheng Q, Xu H, Wang H, et al. [<sup>18</sup>F]SuFEx click chemistry enabled ultrafast late-state radiosynthesis. 2020. ChemRxiv. doi: 10.26434/chemrxiv.10314647.v2
73. Narayanam MK, Toutov AA, Murphy JM. Rapid one-step 18F-labeling of peptides via heteroaromatic silicon-fluoride acceptors. *Org Lett*. 2020;22(3):804–808.
74. Wängler C, Kostikov A, Zhu J, Chin J, Wängler B. Silicon-[18F]fluorine radiochemistry: basics, applications and challenges. *Appl Sci*. 2012;2(2):277–302.
75. IBA Group. Synthera+ V03 brochure. Last updated November 2017. Accessed November 4, 2020. [https://iba-radiopharmasolutions.com/sites/default/files/2020-08/cbr\\_synthera\\_mde\\_v3\\_r01.pdf](https://iba-radiopharmasolutions.com/sites/default/files/2020-08/cbr_synthera_mde_v3_r01.pdf)

76. Gonzalez C, Sanchez A, Collins J, et al. The 4-N-acyl and 4-N-alkyl gemcitabine analogues with silicon-fluoride-acceptor: application to  $^{18}\text{F}$ -radiolabeling. *Eur J Med Chem.* 2018;148:314–324.
77. Chao PH, Lazari M, Hanet S, Narayanam MK, Murphy JM, van Dam RM. Automated concentration of [ $^{18}\text{F}$ ]fluoride into micro-liter volumes. *Appl Radiat Isot.* 2018;141:138–148.
78. Ha N. Microfluidics for the analysis and synthesis of radiopharmaceuticals. Doctoral dissertation, University of California Los Angeles, Los Angeles, CA, USA. 2018.
79. Chao PH-S. Novel microfluidic technologies for the concentration of radionuclides and radiotracers for positron emission tomography. Doctoral dissertation, University of California Los Angeles, Los Angeles, CA, USA. 2019.
80. Nelson WC, Yen M, Keng PY, et al. High pressure EWOD digital microfluidics. In: *Proceedings of the 16th International Solid-State Sensors, Actuators and Microsystems Conference (TRANSDUCERS)*. Beijing, China. June 5-9, 2011:2932–2935.
81. Rios A, Wang J, Chao PH, van Dam RM. A novel multi-reaction microdroplet platform for rapid radiochemistry optimization. *RSC Adv.* 2019;9(35):20370–20374.
82. Jones J, Rios A, Chao P, et al. High-throughput microdroplet radiochemistry platform to accelerate radiotracer development. *Journal of Labelled Compounds & Radiopharmaceuticals*; 2019:S350–S351.
83. Wang J, Rios A, Lisova K, Slavik R, Chatziioannou AF, van Dam RM. High-throughput radio-TLC analysis. *Nucl Med Biol.* 2020; 82-83:41–48.
84. Orlovskaya V, Antuganov D, Fedorova O, Timofeev V, Krasikova R. Tetrabutylammonium tosylate as inert phase-transfer catalyst: the key to high efficiency  $\text{S}_{\text{N}}2$  radiofluorinations. *Appl Radiat Isot.* 2020;163:109195.
85. Dooraghi AA, Carroll L, Collins J, van Dam RM, Chatziioannou AF. ARAS: an automated radioactivity aliquoting system for dispensing solutions containing positron-emitting radioisotopes. *EJNMMI Res.* 2016;6(1):22.
86. Chao PH, Collins J, Argus JP, Tseng WY, Lee JT, van Dam RM. Automatic concentration and reformulation of PET tracers via microfluidic membrane distillation. *Lab Chip.* 2017;17(10): 1802–1816.
87. Ismail R, Irribarren J, Javed MR, Machness A, van Dam RM, Keng PY. Cationic imidazolium polymer monoliths for efficient solvent exchange, activation and fluorination on a continuous flow system. *RSC Adv.* 2014;4(48): 25348–25356.